

Contents

Editorial 1

News

Changes to the operational forecasting system..... 2

New items on the ECMWF website..... 2

71st Council session on 25–26 June 2009 3

EUMETNET's 'Oslo Declaration' 3

Operational assimilation of Indian radiosondes 4

Assimilation of IASI in NWP 5

Goodbye GEMS – Hello MACC..... 6

Ocean waves at ECMWF 7

ECMWF Annual Report for 2008..... 7

Forecast Products Users' Meeting, June 2009..... 8

Diagnostics of data assimilation system performance 9

Meteorology

EPS/EFAS probabilistic flood prediction for Northern Italy: the case of 30 April 2009 10

NEMOVAR: A variational data assimilation system for the NEMO ocean model 17

Improvements in the stratosphere and mesosphere of the IFS 22

The direct assimilation of cloud-affected infrared radiances in the ECMWF 4D-Var 32

General

Peer reviewed publications in 2008 39

ECMWF Calendar 2009..... 40

ECMWF publications..... 40

Index of past newsletter articles..... 41

Useful names and telephone numbers within ECMWF..... 43

Publication policy

The *ECMWF Newsletter* is published quarterly. Its purpose is to make users of ECMWF products, collaborators with ECMWF and the wider meteorological community aware of new developments at ECMWF and the use that can be made of ECMWF products. Most articles are prepared by staff at ECMWF, but articles are also welcome from people working elsewhere, especially those from Member States and Co-operating States. The *ECMWF Newsletter* is not peer-reviewed.

Editor: Bob Riddaway

Typesetting and Graphics: Rob Hine

Any queries about the content or distribution of the *ECMWF Newsletter* should be sent to Bob.Riddaway@ecmwf.int

Contacting ECMWF

Shinfield Park, Reading, Berkshire RG2 9AX, UK

Fax:+44 118 986 9450

Telephone: National0118 949 9000

International+44 118 949 9000

ECMWF website<http://www.ecmwf.int>

EDITORIAL

Enhancing the Archive System

The ease of access to data is fundamental to the success of ECMWF and in particular to the productivity of its research staff. The ECMWF archive system combines a large, comprehensive collection of meteorological data with a high-performance data management and delivery system. This unrivalled combination has become one of ECMWF's most important assets.

The capability offered by the archive system is both valued and strongly supported by the ECMWF Council. At its June 2009 session, the Council authorised the Director to enter into an eight-year call-off contract with Sun Microsystems Ltd for the provision of automated tape libraries and tape drives. By early 2010, three SL8500 automatic tape libraries (ATLs) will have been installed. The libraries will be interconnected, with each library having fifty tape drives and being capable of holding 10,000 tape cartridges. Each single cartridge will be able to hold up to one terabyte of (uncompressed) data. Additional ATLs and tape drives will be installed in subsequent years to keep pace with the growth of the archive. The equipment procured under this contract will replace the ageing STK tape silos. The migration of the data from the old to the new system will be transparent from a user's point of view.

ECMWF's archive system has always been highly appreciated by its users; from the early days, when the amount of data was measured in tens of gigabytes to today, where over ten petabytes of data is archived. In the beginning the archive consisted of files residing on magnetic tape and it was up to the individual user to keep track of the data on these tapes. Very early on it was recognised that this paradigm was not sustainable and so MARS (Meteorological Archival and Retrieval System) was created. MARS was the first system in NWP centres worldwide that used meta-data to enable users to access data using a language tailored towards meteorological terms (e.g. temperature, pressure and grids) rather than reading a particular set of files from a particular set of tapes. ECFS (ECMWF File System) was designed to complement MARS, appearing to the user as a remote general-purpose file system.

The Convention establishing ECMWF specifies the objectives of the Centre: these objectives include specifically the collection and storage of meteorological data. The architecture of the data handling system makes it relatively easy to support new data types and enables an efficient management of large data volumes. The various reanalysis data sets, the TIGGE archive and YOTC (Year of Tropical Convection) data are examples of information that is very widely used by research communities located throughout the world.

Registered users from the ECMWF Member States and Co-operating States are given comprehensive access to ECMWF's archive. As such, the archive held at ECMWF is not only valuable to scientists residing at ECMWF but it is also an important asset to the entire European atmospheric community.

Walter Zwiefelhofer

Changes to the operational forecasting system

DAVID RICHARDSON

New cycle (Cy35r3)

A new cycle of the ECMWF forecast and analysis system, Cy35r3, is undergoing pre-operational testing. Changes for this cycle include:

- Addition of GOME-2 total column ozone data from the METOP satellite.
- Assimilation of cloud-affected radiances for infra-red instruments.

- Improved assimilation of satellite channels that are sensitive to the land surface.
- Assimilation of total column water vapour data from the MERIS instrument.
- Variational bias correction for ozone satellite data.
- Improved quality control (using Huber norm) of conventional observations.

- Improved background-error statistics for humidity, new humidity formulation in 4D-Var.
- Weak-constraint 4D-Var taking into account systematic model errors in the stratosphere.
- Non-orographic gravity wave scheme.
- New trace gas climatology.
- Further revision of the snow scheme.
- Revised stochastic physics (model perturbations) for EPS.

New items on the ECMWF website

ANDY BRADY

New model simulated satellite images

A new product is available from our deterministic forecast – simulated infra-red and water vapour geostationary satellite images from the T799 deterministic forecast. The product is available out to five days.

- www.ecmwf.int/products/forecasts/d/charts/medium/deterministic/simulated/sim/

New wave forecast charts

A new page is available for our ocean wave products including an extended set of verification products for the wave forecasts. A comparison with other operational forecast centres is also available.

- www.ecmwf.int/products/forecasts/wavecharts/

Funding and Member States' contributions

The scale of contribution of each Member State and Co-operating State is according to its Gross National Income (GNI) and is revised every 3 years. The contributions to the ECMWF Budget have been updated for 2009.

- www.ecmwf.int/about/funding/

T-PARC – THORPEX Pacific Asian Regional Campaign

T-PARC is a two-phase multi-national field experiment. The first and primary phase (Summer T-PARC) ran from August to October 2008. The second phase (Winter T-PARC) ran from mid-January through to March 2009. In both phases the geographical focal point is the North Pacific and surrounding countries. During Summer T-PARC the main meteorological focus was tropical cyclones and extra-tropical transition – most activity therefore was in the western North Pacific region. In Winter T-PARC downstream impacts over North America are more relevant so activity then covers the whole of the North Pacific region, but with less emphasis on the tropics.

- www.ecmwf.int/research/WMO_projects/TPARC/index.html

ECMWF/EUMETSAT NWP-SAF Workshop on the 'Assimilation of IASI in NWP'

The ECMWF/EUMETSAT NWP-SAF Workshop on the 'Assimilation of IASI in NWP' was held from 6 to 8 May 2009. The presentations are available.

- www.ecmwf.int/newsevents/meetings/workshops/2009/IASI_data/index.html

ECMWF Workshop on 'Diagnostics of data assimilation system performance'

The Workshop on 'Diagnostics of data assimilation system performance' was held from 15 to 17 June 2009. The presentations are available.

- www.ecmwf.int/newsevents/meetings/workshops/2009/Diagnostics_DA_System_Performance/

MACC scientific and technical training workshop

ECMWF will host the first Scientific and technical training workshop for the MACC (Monitoring Atmospheric Composition and Climate) project from 11 to 15 January 2010.

- www.ecmwf.int/newsevents/meetings/workshops/2010/MACC/

SAFER (Service and Applications for Emergency Response)

In the frame of GMES initiative (Global Monitoring for Environment and Security), the SAFER project aims at implementing preoperational versions of the Emergency Response Core Service. SAFER will reinforce European capacity to respond to emergency situations.

- www.ecmwf.int/research/EU_projects/SAFER/

71st Council session on 25–26 June 2009

MANFRED KLÖPPEL

On the invitation by its President, Dr Adérito Vicente Serrão from Portugal, the ECMWF Council held its 71st session in Ponta Delgada in the Azores on 25–26 June 2009.

Besides several decisions made on financial and staff matters (such as adoption of Reports from the Co-ordinating Committee on Remuneration), the main results of this session were as follows.

● **Amendments to the Convention.**

Good progress had been made with the ratification process within Member States. If such progress is maintained, the amended Convention could come into force by the end of 2009.

● **Co-operation Agreements.** The Council unanimously authorised the Director to conclude a Co-operation Agreement with the Government of Bulgaria and to renew the Co-operation Agreement with the African Centre of Meteorological Application for Development (ACMAD).

● **Extension of an existing licence agreement.** The Council unanimously approved the extension of the existing licence agreement between ECMWF and EUROBRISA, allowing Brazil's Centro de Previsão de Tempo e Estudos Climáticos (CPTEC) to receive real-time, multi-model, seasonal forecasts from ECMWF until June 2012.



● **GMES (Global Monitoring for Environment and Security).** The Council agreed that ECMWF should continue to play an active role as coordinator of and main contributor to the atmosphere network, as foreseen in the European Commission's communication issued in November 2008.

● **Registered Partnership.** The Council adopted the same text as already adopted by the Council of Europe on registered partnerships, to be implemented at ECMWF under a new Article of the Staff Regulations.

● **Financial Matters.** The Council took note of the Auditor's Report regarding the financial year 2008 and gave discharge to the Director in respect of the implementation of the budget for 2008. The Council also considered preliminary estimates of Member States' contributions to the 2010 budget.

● **Data Handling System.** The Council unanimously authorised the Director to enter into a contract for the renewal of the automated tape library with Sun Microsystems Ltd., and on a call-off basis for 8 years from the start of the contract.

● **Oslo Declaration.** The Council unanimously adopted the 'Oslo Declaration' as a guideline for formulating ECMWF's data policy.

● **Use of ECMWF Products.** The Council unanimously adopted the revised standard licence agreement for use of ECMWF Products and the revised 'Rules governing the distribution and dissemination of ECMWF real-time products'.

Prof Erland Källén, who took up his post as Head of Research at ECMWF on 6 July 2009, attended the Council giving a presentation about 'Using re-analyses to understand arctic warming'.

EUMETNET's 'Oslo Declaration'

BOB RIDDAWAY

EUMETNET is a network of 26 European National Meteorological Services (NMHSs). It provides a framework for organising co-operative programmes involving basic meteorological activities. At a meeting in Oslo on 26–27 March the EUMETNET Council reviewed the current policies concerning

meteorological data. This led to the adoption of the 'Oslo Declaration' which encapsulates the points on which a common position was agreed during the meeting.

At its meeting on 25–26 June 2009, the ECMWF Council adopted the 'Oslo Declaration' as a guideline for formulating ECMWF's data policy.

The following is the 'Oslo Declaration'.

At their Meeting in Oslo, Norway on 26–27 March 2009 to discuss data policy matters, the directors of the EUMETNET National Meteorological Services, recognising that:

– Significant investments and sustained funding are necessary at national level to maintain and develop the basic components of the European Meteorological Infrastructure required to fulfil the general needs of the

public, the decision makers and the European economy;

- National governments can meet this basic requirement under different funding policies associated to different economic models for NMHS and variations in data policies;
 - Although their NMHS operate under different official mandates and economic models and accordingly run different activity portfolios, all are committed to provide the best possible contribution to protection of life and property under their Public Weather Service mission, directed at national authorities and the general public;
 - The internet and the web technologies have changed radically the expectations from the general public and the access to and possible sharing and use of data, products and services;
 - The ongoing development of the WMO Information System will take advantage of these innovative technologies;
 - The legal framework provided by the EU including the INSPIRE and PSI Directives places new expectations on the way the NMHSs provide their services
- have reached consensus on the following:

1) Data policies of the EUMETNET

members, ECMWF and EUMETSAT and the related development of on-line services, should:

- facilitate direct access to basic meteorological data and products on a non discriminatory basis, under well-documented licensing conditions, in compliance with relevant international and national regulations and with WMO resolutions;
 - be harmonized as far as possible to achieve greater transparency and improve accessibility for re-users within the constraints of the legal frameworks and respective economic models of the NMHS, taking into account relevant discussions in the context of EUMETNET, ECMWF, ECOMET and EUMETSAT bodies.
- 2) The evolution of the basic output of NMHS, as a result of advances in science and in observation and numerical weather prediction and technology, should lead to regular reviews at NMHS level, and, when appropriate, to progressive expansions of:
- their set of “Essential” data and products made available on a free and unrestricted basis;
 - their catalogue of data and products licensed for re-use by the private sector, under the PSI directive where applicable.

3) In the same spirit, NMHS should also consider adapting their licensing conditions with the objective of delivering more information per price unit, if financial constraints allow.

4) The EUMETNET members should continue to develop, individually and jointly through EUMETNET programmes, on line services giving user-friendly access to these catalogued data and products, in order to facilitate further the re-use of public meteorological information and to maximise the societal benefits.

5) In the spirit of the INSPIRE directive, the EUMETNET members should expand the set of graphical products accessible free of charge to the public for general purposes, through the viewing services of their respective web sites, whilst continuing to license as appropriate the underlying digital data and products.

6) In the context of GMES, meteorological data and products required by the operators of the GMES Core Services to deliver new, non meteorological public good services, could be licensed to them at no information cost to fulfil their production duties, subject to commitment from EU and national authorities to fund these Core Services on a sustainable basis.

Operational assimilation of Indian radiosondes

ANTONIO GARCIA-MENDEZ

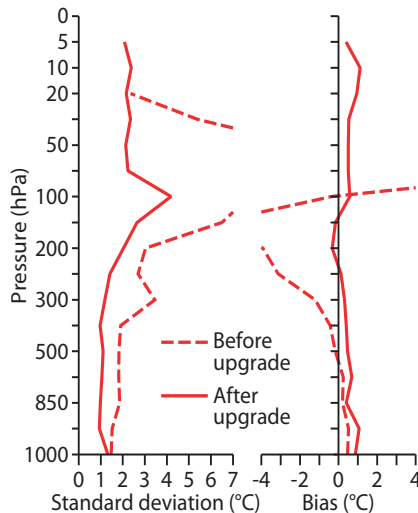
For many years, temperature reports from Indian radiosondes have generally been blacklisted in the ECMWF operational data assimilation because of their inconsistency and relatively low quality. The Indian Meteorological Department has now begun a programme to update its radiosonde network to use the French Modem MK2K GPSonde. The first phase of this plan can be seen in the table.

The first five sites were upgraded in March to April 2009. The observations from these stations were carefully monitored at ECMWF during the

Station name	Identifier	Location	Date commissioned
Thiruvananthapuram	43371	8.79°N, 76.57°E	9 March 2009
Mohanbari	42314	27.79°N, 95.01°E	9 April 2009
Chennai	43279	12.59°N, 80.11°E	13 April 2009
Port Blair	43333	11.39°N, 92.44°E	16 April 2009
Minicoy	43369	8.16°N, 73.03°E	23 April 2009
Goa	43192	15.79°N, 73.49°E	12 May 2009
Hyderabad	43128	17.77°N, 78.28°E	5 May 2009
Visakhapatnam	43150	17.92°N, 83.18°E	18 May 2009
Patna	42492	25.86°N, 85.06°E	21 May 2009
Srinagar	42027	34.55°N, 74.50°E	24 May 2009

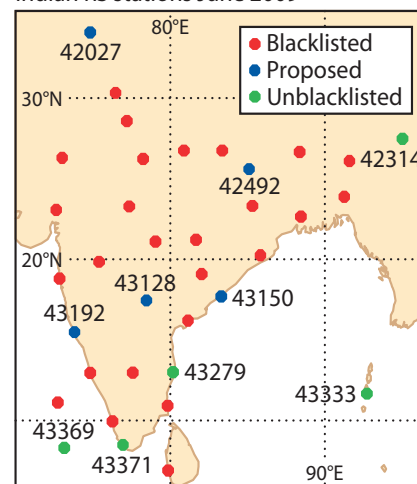
following weeks to assess the performance using the new equipment. In all cases the quality change was remarkable and the ECMWF operational monitoring showed that these all now consistently provide good quality temperature soundings. The number and quality of humidity and wind observations also improved, enabling the ECMWF analysis system to use these data more extensively than the data from the previous radiosondes.

On 12 May, these five sites were removed from the ECMWF blacklist and their observations are now assimilated in the operational system. Five more sites were upgraded during May. After a short period of monitoring that confirmed the quality and consistency of the new systems, these sites were also removed from the blacklist and included in the assimilation. As more stations are upgraded, they too will be assimilated after short periods of monitoring.



Upgrade of Indian radiosondes. The figure shows the statistics for a station in the extreme South of India (Thiruvananthapuram) that was upgraded on 9 March 2009. Shown are the vertical statistics for standard deviation (left) and bias (right) between the temperature observations and the ECMWF analysis for periods before the upgrade (31 January to 8 March) and after the upgrade (9 March to 23 May).

Indian RS stations June 2009



The Indian radiosonde network. Five stations were upgraded to use Modem M2K2 GPS sondes in March to April and were assimilated at ECMWF from 12 May (green dots); five more stations were upgraded during May and assimilated at ECMWF from 16 June (blue dots). The remaining stations in the Indian network have not yet been upgraded (red dots), and temperatures from these sites are not used at ECMWF.

Assimilation of IASI in NWP

TONY MCNALLY

A Workshop on the assimilation of IASI in NWP, co-sponsored by the EUMETSAT NWP-SAF (Satellite Application Facility) and organized by ECMWF, was held at ECMWF from 6 to 8 May 2009.

IASI (Infrared Atmospheric Sounding Interferometer) was launched onboard MetOp in October 2006 and is the first hyperspectral instrument carried by an operational satellite. By measuring atmospheric radiation in many thousands of different channels IASI provides unprecedented information on temperature, humidity and atmospheric composition. IASI radiances have been incorporated into ECMWF's operational forecasting system since June 2007.

The 40 participants at the workshop represented operational NWP centres, satellite data providers and academic institutions. The purpose of the workshop was to:

- Gather experts to assess the progress that has been made in the



exploitation of IASI and identify key areas for future development.

- Provide training through a sharing of experiences among data providers and data users.

The workshop followed a format of one and a half days of lectures after which the participants broke out into three parallel working groups.

In the group dealing with IASI instrument validation and radiative transfer modelling there was a consensus that the IASI spectra were

calibrated extremely accurately and that the procedures that led to this exceptional performance should be documented and applied to future missions. The important role of validation field campaigns, NWP radiance monitoring and inter-comparison activities such as CSICS (Global Space-Based Intercomparison System) was highlighted. It was noted that the high quality of the IASI observations placed very stringent requirements upon the accuracy of

radiative transfer models. In particular the group stressed the need for long-term support of improvements in spectroscopy and line-by-line modelling.

The fact that all NWP centres using IASI data reported significant impacts on forecasting skill was noted by the working group dealing with IASI assimilation. Indeed some centres assess the impact of IASI as being greater than that of any other single satellite instrument. It was noted that the speed at which IASI was implemented in a number of operational systems was partly due to the very

good experience gained with AIRS data. The group acknowledged that IASI was still significantly underused and suggested that developments aimed at treating data over land and cloud affected radiances should lead to future improvements.

The application of IASI data to the estimation of trace gas and other chemical species was dealt with by the working group on environmental monitoring. During the workshop the wealth of information provided by IASI for constituent retrieval was documented. The group noted that this activity was the most demanding

on data quality and stressed that any future degradation to achieve compression for data transfer should be avoided.

More detailed reports from the workshop will appear in the forthcoming proceedings, but in the meantime the presentations are available for viewing on:

- www.ecmwf.int/newsevents/meetings/workshops/2009/IASI_data/

In conclusion ECMWF would like to thank EUMETSAT for their support and thank the participants for making the workshop and extremely interesting and successful event.

Goodbye GEMS – Hello MACC

ADRIAN SIMMONS

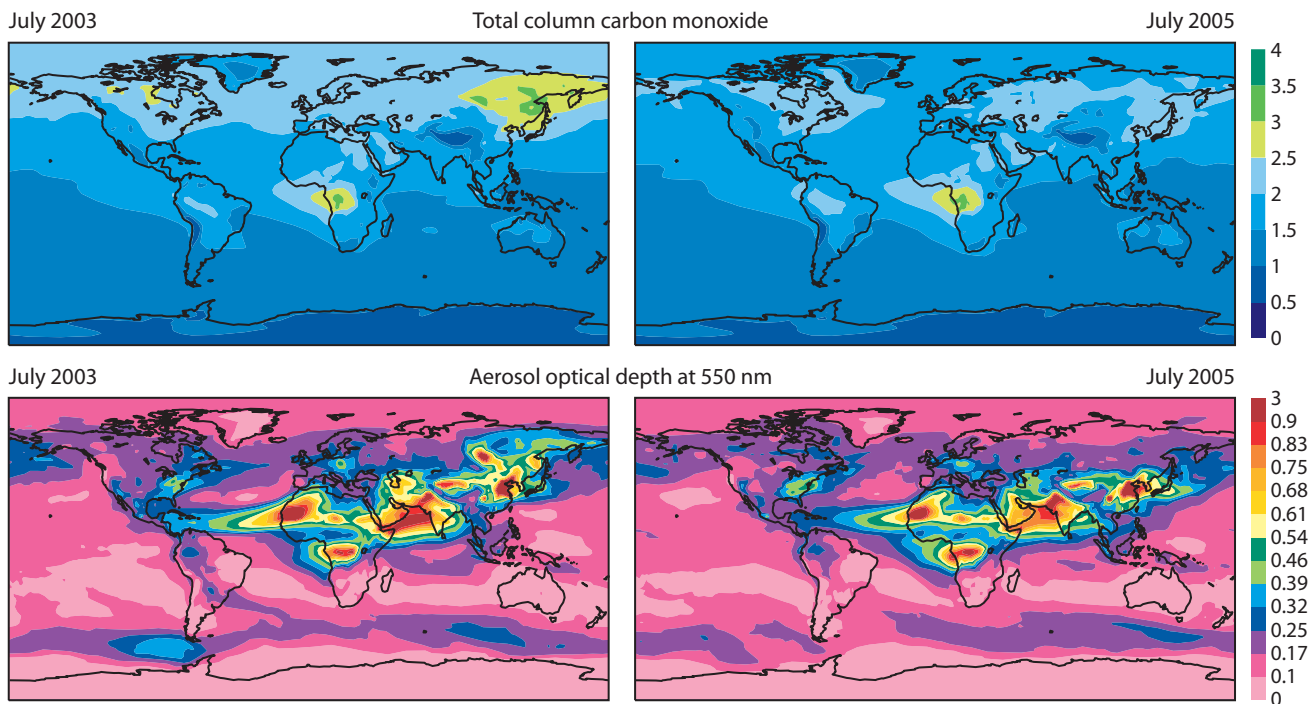
The EU-funded GEMS project ran from 1 March 2005 to 31 May 2009. Operation and improvement of the systems developed during GEMS is continuing in a new EU-funded project MACC – Modelling Atmospheric Composition and Climate.

The EU-funded GEMS project started on 1 March 2005 under the

leadership of the late Tony Hollingsworth, and came to an end on 31 May 2009. GEMS achieved its objectives of building and demonstrating the operation of global and regional analysis and modelling systems that monitor and predict variations in atmospheric constituents that force climate change and influence air quality, ultraviolet radiation and solar energy resources. In total, 32 partner

organizations were involved, with ECMWF developing and operating the core global component and supporting the regional component with data handling, validation and display of results.

Most of the partners in GEMS will continue in MACC, but the project will increase in size to 48 partners as activities are included from a related ESA-funded project called PROMOTE



GEMS aerosol and carbon monoxide analyses. These analyses show large differences over north-eastern Asia between July 2003 and July 2005, due to much greater fire activity over Siberia in 2003. MACC will provide both daily analyses and forecasts and a reanalysis for 2003–2010.

(Protocol Monitoring for the GMES Service Element: Atmosphere), which concludes later in 2009.

MACC will adopt a more operational approach to the running of its systems and have a stronger focus on the interface with users and downstream

service providers. It will run from 1 June 2009 until late in 2011, when it should be ready to emerge as a fully operational atmospheric service under the European Union's GMES (Global Monitoring for Environment and Security) programme.

Pending the establishment of a capability for product display and delivery from the MACC web pages, the GEMS web pages are being used to present the results from MACC's operation of global and regional systems.

Ocean waves at ECMWF

PETER JANSSEN

Prediction of the maximum wave height of extreme events is of tremendous benefit to the marine world. A considerable amount of progress in wave modelling has been achieved in the past 20 years or so and there are definite reasons for further development. A global wave prediction model has been in operations at ECMWF since 1992.

Since then, the original WAM forecasting system has undergone significant enhancements including:

- Assimilation of altimeter wave height data.
- Two-way interaction of wind and waves.
- Increase in spatial resolution from 330 km to 25 km.

In addition there has been a massive improvement in the ability

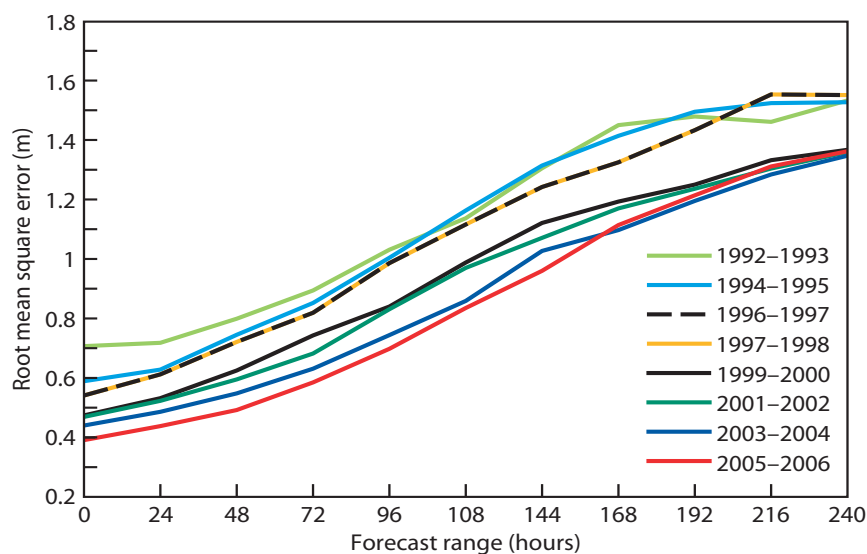
to forecast the driving surface wind fields. These developments have resulted in a significant improvement in the accuracy of the wave height forecasts. In addition the ECMWF forecasts of wave height outperform those from other operational centres.

More detail about these developments along with information about the ensemble prediction of ocean waves, extreme wave forecasting and the use of satellite observations can be found in the leaflet 'Ocean waves at ECMWF'. The leaflet can be found at:

- www.ecmwf.int/about/information_leaflets/Ocean-waves-English.pdf

Also information about wave forecasting is available from a new website that has been launched recently: see 'Ocean wave forecast' at:

- www.ecmwf.int/products/forecasts/d/charts/



Improvement in the accuracy of wave height forecasts. The improvement in accuracy is illustrated by the reduction in root mean square error of forecast wave height verified against independent observations from buoys for winters (October to March) since 1992/93. The forecasts are from 12 UTC each day. These results can be interpreted as indicating a gain of more than two days in the accuracy of the forecasts.

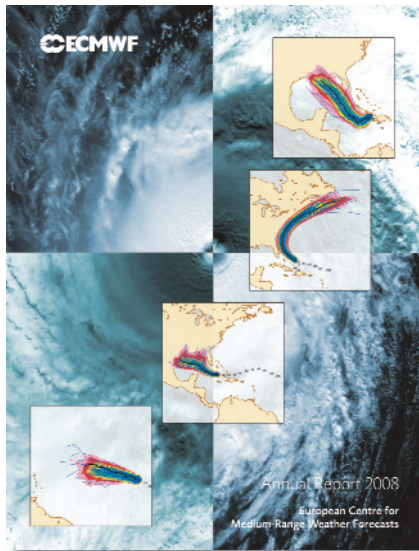
ECMWF Annual Report for 2008

BOB RIDDAWAY

The *ECMWF Annual Report 2008* has been published. It is intended to be an important way of maintaining the flow of information to all the people and institutions that have an interest in ECMWF.

The report draws attention to some of the key events of 2008 that affected operational activities.

- **Revised production schedule.** A revised production schedule was introduced with the result that products have become available from 10 to 15 minutes earlier than before, depending on the type of product. *29 January.*
- **Development of a unified forecasting system.** The Monthly Forecasting System was integrated with the medium-range Variable Resolution Ensemble Prediction System (VarEPS). *11 March.*
- **Availability of ERA-Interim products.** ERA-Interim reanalysis products for the years 1989–1998 were made available for research and education with a latitude/longitude resolution of 1.5°. *10 April.*
- **Provision of marine products for WMO Members.** A range of marine forecast products to support severe weather marine forecasting was made available to WMO Members. *15 April.*
- **Assimilation of GPS radio occultation.** GPS radio occultation data from the GNSS Receiver for Atmospheric Sounding (GRAS) instrument onboard EUMETSAT's MetOp satellite was actively assimilated at ECMWF. *28 May.*
- **Implementation of IFS Cycle 33r1.** A new IFS cycle was implemented with important changes to the wave model,



some retuning of the representation of physical processes and improved use of satellite data. 3 June.

● **Monitoring altimeter wind and wave data from the Jason-2.** ECMWF started to receive and monitor altimeter wind and wave data from the Jason-2 satellite. 9 September.

● **Implementation of IFS Cycle 35r1.** A new IFS cycle was introduced with several changes to the representation of physical processes, such as improvements to the handling of melting snow and a new sea surface temperature analysis product. 30 September.

● **Usage of the HPCF.** Member States' usage of the ECMWF High Performance Computer Facility resources reached a new milestone with 100 million units being exceeded in 2008. 22 December.

As well as describing how research and operational activities combine to bring high quality research through to enhancing operational capabilities, the *Annual Report* also includes information about the following.

● **Performance of the forecasting systems.** The performance of the forecasting systems remained at a high level throughout the year with several severe weather events successfully forecast several days in advance.

● **High Performance Computing Facility (HPCF).** The existing HPCF, one of the most powerful in Europe, continued to provide a very good service to users. In addition preparations have been made for the installation of the new super-computer provided by IBM UK Ltd.

● **Workshops and training courses.** A variety of workshops were held that help shape the research and development activities at ECMWF. Also ECMWF contributed to the development of meteorological expertise within Europe by running a variety of training courses.

● **Collaborative research programmes.** ECMWF participated in a number of collaborative research programmes run by the European Union and WMO. The outcome of these programmes helps improve global forecasting, develop new technologies and improve atmospheric monitoring.

● **Amended Convention.** By the end of 2008, 13 Member States had notified acceptance of the amendments to the Convention. Also the Council authorised the start of negotiations with a view to increasing the number of States that have full membership of ECMWF.

Dominique Marbouty, ECMWF Director, outlined the key developments in his foreword to the *Annual Report* and finished by stating that:

“The last year has been very successful and the foundations have been laid to build upon the past achievements of ECMWF in the coming years. As in the past, the success of ECMWF will continue to be based on the quality of the staff and the fruitful relationship between ECMWF and its Member States.”

The *Annual Report* can be downloaded from:

● www.ecmwf.int/publications/annual_report/

Forecast Products Users' Meeting, June 2009

DAVID RICHARDSON

ECMWF organizes an annual meeting of users of its medium range and extended range products. The purposes of the meetings are to:

● Review the development of the operational system and to discuss future developments including forecast products.

● Give users of the ECMWF forecasts the opportunity to discuss their experience with and to exchange views on the use of the medium-range and extended-range products

The 2009 Forecast Product Users Meeting took place at ECMWF from 10 to 12 June, with 42 participants representing 17 National Meteorological

Services and 9 commercial customers in the Member States and Co-operating States.

Two new cycles of the operational assimilation and forecasting system have been implemented since the last meeting. These changes and the impact on the forecasts were presented and included several modifications to the physics, such as a revised snow scheme, a new sea surface temperature analysis product, and direct 4D-Var assimilation all-sky of microwave imagers. Plans for future developments of the ECMWF forecasting system were also presented. These include:

● A substantial increase in horizontal resolution during 2009 for the data

assimilation, deterministic forecast and EPS.

● Revision of the initial perturbations and stochastic physics for the EPS.

● Further improvements to the data assimilation and model physics.

The Member States and Co-operating States representatives presented their use of ECMWF products and their experience with the forecasts in the past year. They were generally very happy with the quality of the forecasts. It was emphasised that ECMWF products are widely used in the forecast offices, and are especially useful in providing guidance for early warnings of potential high-impact and extreme events. Users noted the improvements to the snow forecasts

in the last winter, but also highlighted the issues about the snow cover and night-time temperature biases that affected Central Europe in the past winter. However, an extreme cold spell affecting Germany had been well predicted two weeks in advance.

New products that have been implemented this year include simulated infra-red and water vapour geostationary satellite images from the deterministic forecast. Member States confirmed their requirements for the new products that are in development at ECMWF, including tracking of extra-tropical cyclonic

features, strike probability forecasts for tropical cyclones that develop during the forecast (for both medium-range and monthly forecast) and revision of the EPS clustering. Representatives presented some requests for additional products, mainly to provide more direct information on weather parameters such as visibility, cloud base height and low level winds.

The forecast products displayed on the ECMWF web site are increasingly used during the forecasters' routine duties in the Member States. There was confirmation of their require-

ments for the ECMWF web to provide a highly available service and to enhance interactivity, including new features such as zoom, pan and overlay of charts, and more choice of parameters for EPSgrams. ECMWF's plans for a re-engineered web service to provide such forecast products for the Member States and Co-operating States were reviewed and discussed.

The presentations and summary from the meeting are available on the ECMWF website:

- www.ecmwf.int/newsevents/meetings/forecast_products_user/Presentations2009/

Diagnostics of data assimilation system performance

CARLA CARDINALI

The Workshop on 'Diagnostics of data assimilation system performance' was held at ECMWF from 15 to 17 June 2009.

Over the last years data assimilation schemes have evolved into complicated systems with millions of degrees of freedom and handling massive amounts of observations. Effective monitoring of these systems is required and emerging techniques

are now rapidly developing at most NWP centres. The review of the various methodologies and their effectiveness in diagnosing the impact of observations in NWP was suitably timely.

The workshop considered all available techniques to measure the performance of the NWP assimilation system. The impact of observations on the assimilation and the short-range forecast has been assessed through different diagnostic tech-

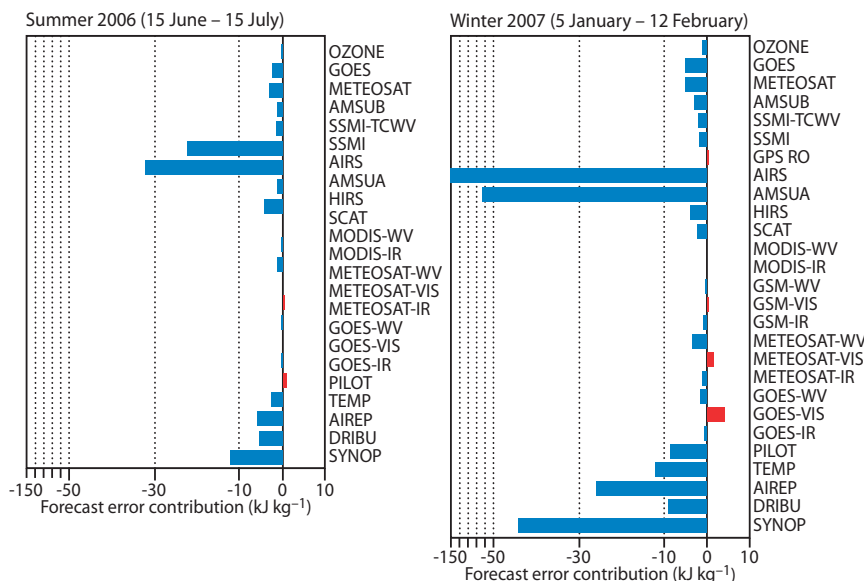
niques. In particular, methodologies that evaluate the analysis optimality were presented.

Over the last few years, adjoint techniques have also been used to assess the impact of observations on the short-range forecast. This methodology was described and compared with the more commonly, so far used, Observation System Experiment technique. The use of adjoint technique to measure the impact in the short-range forecast of the other analysis input parameters was also presented. Interesting presentations showed different methodologies to assess model bias, for example through re-analysis experiments or projection of analysis increments and short-range forecast error onto the most important modes of the numerical model.

Workshop lectures were by invitation only. However, a call for poster was introduced to give the opportunity to the younger scientists to participate and illustrate their work. The workshop proceeding will be issued before the end of the year.

The presentations given at the workshop along with the posters can be found at:

- www.ecmwf.int/newsevents/meetings/workshops/2009/Diagnostics_DA_System_Performance/



Monitoring ECMWF's data assimilation system. Contribution of the various components of the observing system to the 24-hour forecast error for a period in the summer of 2006 (left panel) and a period in the winter of 2007 (right panel). Negative (positive) values are associated with a decrease (increase) of forecast error due to different component of the observing system. Globally the observations contribute to decrease in the forecast error.

EPS/EFAS probabilistic flood prediction for Northern Italy: the case of 30 April 2009

ROBERTO BUIZZA, FLORIAN PAPPENBERGER,
PETER SALAMON, JUTTA THIELEN, AD DE ROO

ENSEMBLE hydrological predictions generated by the European Union Joint Research Centre European Flood Alert System (JRC EFAS) driven by the ECMWF Ensemble Prediction System (EPS) have been used to assess the risk of flooding of the Po' river at the end of April 2009. This case illustrates the added value of using probabilistic flood predictions to signal the possible occurrence of flooding, and confirms statistically-based results published in the scientific literature. It shows that the key advantage of ensemble prediction systems, compared to systems that rely on one single forecast, is that they can be used not only to identify the most likely outcome, but also to assess the probability of occurrence of extreme/rare events.

Medium-range ensemble prediction systems are today part of the operational suite at many meteorological centres. Nine centres (in Australia, Brazil, Canada, China, England, Japan, Korea and the USA; see, for example, Buizza et al., 2008) run global, medium-range ensemble prediction systems, and many regional centres are running limited area ensemble prediction systems (e.g. in Australia, England, France, Germany, Italy, Norway and Spain). The past decade has seen an increased use of ensemble forecasts; see, for example, the work done within the DEMETER project on establishing the utility of coupled multi-model ensemble forecasts, in particular in the agriculture and health sectors; www.ecmwf.int/research/demeter/.

Another area where the value of an ensemble approach has been widely recognized is hydrology, which has seen several institutions developing and testing ensemble-based flood prediction systems that use ensemble weather forecasts as initial and boundary conditions (see, for example, the work done within the HEPEX project, Thielen et al., 2008). One of these hydrological ensemble systems for flood prediction is EFAS, developed and successfully implemented by JRC in Ispra, Italy.

Probabilistic prediction of severe water level conditions with EPS/EFAS

The EPS/EFAS flood prediction system runs twice-a-day at JRC using forecasts of the weather variables required

by the hydrological model to predict river discharge levels. EFAS probabilistic forecasts use data from the ECMWF EPS as initial and boundary weather conditions.

The ECMWF EPS

The EPS has changed several times since its implementation in 1992 (see Palmer et al., 2007 for more details). Since 11 March 2008, the ECMWF EPS runs twice-a-day, at 00 and 12 UTC, with a variable resolution (Buizza et al., 2006 and Vitart et al., 2008). It includes 51 members: one starting from unperturbed initial conditions (defined by interpolating the high-resolution T799L91 analysis to the ensemble resolution) and 50 members starting from perturbed initial conditions.

The perturbed initial conditions are constructed as a linear combination of the perturbations with the fastest growth over a 48-hour period, provided by singular vectors computed with a T42L62 model and a total energy norm. The perturbed forecasts are integrated with a stochastic scheme designed to simulate the effect on forecast error of random model errors due to uncertainties in the parametrized physical processes (the stochastic physics).

The 00 UTC EPS is run at T399L62 resolution from day 0 to day 10 with persisted sea-surface-temperature anomalies, and then at T255L62 resolution from day 10 to day 15 (day 32 every Thursday at 00 UTC) coupled with an ocean model. Every Thursday the ensemble is extended to 32 days to cover the monthly forecast range. The 12 UTC EPS has the same configuration as that run at 00 UTC, but uses persisted sea-surface-temperature anomalies also between day 10 and 15, instead of a coupled ocean model.

The JRC EFAS

The European Flood Alert System (EFAS) was launched in 2003 by the European Commission with the aim to increase preparedness for floods in trans-national European river basins (Thielen et al., 2009; Bartholmes et al., 2009). The system being developed has two main objectives:

- ◆ To complement European Member States activities on flood preparedness and to achieve longer early warning times.
 - ◆ To provide the European Commission with an overview of ongoing and expected floods in Europe for improved international aid and crisis management in the case of large transnational flood events that might need intervention on an international level.
- The EFAS prototype that is currently run operationally is set up for the whole of Europe on a 5-km grid. Twice daily it provides the national hydrological centres with

AFFILIATIONS

Roberto Buizza, Florian Pappenberger, ECMWF, Reading, UK
Peter Salamon, Jutta Thielen, Ad de Roo, JRC, Institute for Environment and Sustainability, Ispra, Italy

medium-range ensemble flood forecasting information. In addition, when a high probability for flooding is forecast, the EFAS partners are alerted by e-mail and advised to monitor the development of the situation using the EFAS information system. Currently, forecasts with lead times of 3 to 10 days are achieved through the incorporation of ensemble and single forecasts:

- ◆ Two deterministic weather forecasts from ECMWF and the German Weather Service (DWD).
- ◆ Two sets of ensembles: the medium-range EPS from ECMWF (51 members, 10 days) and the shorter range COSMO-LEPS (16 members, 5 days) provided by the Regional Meteorological Service of Emilia-Romagna (ARPA-SIM), Bologna, Italy.

EPS/EFAS probabilistic predictions for 28–30 April 2009

To illustrate the value of EPS/EFAS probabilistic flood predictions in weather-related risk management, the severe meteorological and hydrological conditions that affected Northern Italy at the end of April 2009 are now discussed. For this example, only precipitation forecasts generated by the ECMWF EPS and the corresponding EPS-driven EFAS flood predictions have been used.

April 2009 was a rather wet period for Northern Italy. Towards the end of the month, river levels were quite high due to springtime rain and the beginning of the snow melting (Northern Italy witnessed very heavy snowfalls during winter 2008/09). On 29 April, Italian newspapers started listing the various damages due to the very high river levels caused by the heavy precipitation that hit this region on the 27th and 28th. It is interesting to read what was reported about this event in a local Italian news paper (*VareseNews* from Ispra).

Po' river flood: the JRC forecast is confirmed

JRC predicted and communicated last Friday the high level reached by the Po river during these days. The news comes from JRC, which runs EFAS, the European Flood Alert System. On the 24th of April, EFAS personnel sent an alert message to the Italian Protection Agency, the Po' river Authority and other partner authorities. EFAS was predicting a high probability that the Po river would reach flood levels from the 27th of April, with peak levels between the 28th and the 29th. The warning was issued 4–5 days before the event, confirming the great potential of the EFAS-based warning system. Since Friday the 24th, EFAS partners could follow the sequence of EFAS predictions, updated every 12 hours, from the JRC web site, via the area that gives them restricted access to the EFAS forecasts (see Figure 1 for the original Italian article).

This newspaper article indicates that users are becoming increasingly familiar with the notion of a probabilistic forecast, and that decisions are made based on probabilistic forecasts.

Vereze News, 29 April 2009.

Piena del Po: confermate le previsioni del Ccr

La piena del Po di questi giorni era stata prevista e annunciata dal Centro Comune di Ricerca (CCR, also named Joint Research Centre, JRC) di Ispra da venerdì scorso. Lo comunica lo stesso centro comunitario che rende nota l'attività svolta da EFAS, il sistema europeo di allerta sulle alluvioni ospitato all'interno dello stesso CCR. Il 24 aprile i responsabili di EFAS hanno inviato la notifica di allerta sulla piena del Po all'Istituto Superiore per la Protezione e la Ricerca Ambientale, alle autorità competenti per le acque del Po e alle organizzazioni nazionali partner per il grande fiume padano. Le previsioni di EFAS infatti prevedevano un'alta probabilità di alluvioni del Po a partire dal 27 aprile, con un picco d'onda tra il 28 e il 29. L'avviso è stato emesso con 4–5 giorni di anticipo, il che conferma il grande potenziale di questo sistema di avvertimento preventivo. A partire da venerdì 24 inoltre i partner italiani dell'EFAS hanno potuto seguire l'andamento delle previsioni, aggiornate ogni 12 ore sull'area ad accesso riservato del sito Internet del sistema.

Figure 1 Extract from VareseNews of 29 April 2009 (see <http://www3.varesenews.it/varese/>).

Figures 2 and 3 show some of the consequences of the high river levels: in Alessandria, one of the main cities of Piemonte, over Northwestern Italy, some areas were flooded and some of the bridges were closed due to the extremely high level of the river Tanaro (Figure 2). In Piacenza, on 30 April one of the Po' river bridges collapsed causing accidents and casualties (Figure 3). The collapse has been linked to the water pressure associated with the extremely high levels of the Po'.

Precipitation forecasts

River flooding was due to the heavy precipitation that affected this region between 27 and 29 April. On the 26th, the upper-level atmospheric flow was characterized by a deep trough positioned over Spain with a southwest-northeast axis that started funnelling hot, moist air towards Northwest Italy. The surface flow was characterized by a weak cyclonic circulation centred on the Balearic Islands. During the subsequent 48 hours, the upper-level trough moved slowly towards Italy with its axis gradually tilting from southwest-northeast towards south-north, and then towards a southeast-northwest direction, while at the surface the cyclonic circulation intensified. This upper level and surface circulation caused heavy precipitation over Italy, especially over the Po' Valley.

Figure 4 shows the areas of heavy precipitation (48-hour accumulated precipitation in excess of 15 mm) given by the 0–48 hour forecast produced by the ECMWF high-resolution model, and the corresponding observed



Figure 2 Alessandria, 29 April 2009. The Tanaro river reaches extremely high levels (photo: A Contaldo, Photonews, available from <http://torino.repubblica.it/>)

La Stampa, 29 April 2009.

La Regione Piemonte «Stato di emergenza dopo la piena». In tutto il Piemonte ci sono stati allagamenti e smottamenti di strade. Situazione difficile oltre che ad Alessandria anche nel Cuneese, nell'Astigiano e in Val d'Ossola. La presidente Mercedes Bresso ha chiesto lo stato di emergenza. Allerta per il Po' invece dalla Protezione civile dell'Emilia-Romagna, dove la piena e' attesa per oggi. La piena in Piemonte, dovrebbe avere una portata stimata sui 7.000 metri cubi al secondo.



Figure 3 Piacenza, 30 April 2009. The collapse of one of the bridges across the Po' (photo: P Caridi, WordPress, available from <http://peppecaridi2.wordpress.com/>).

La Repubblica, 30 April 2009.

Crolla un'arcata, precipitano 4 macchine. Grave un automobilista ricoverato in rianimazione. Piena del Po', crolla ponte a Piacenza Le auto finiscono in acqua: 4 feriti Piena del Po', crolla ponte a Piacenza. Un'arcata ha ceduto alla furia della piena del fiume e l'asfalto si è piegato verso l'acqua trascinando quattro auto. La strada si è piegata in una sorta di "v".

precipitation. These two maps show that the whole of Italy was affected by heavy precipitation (note that the figures have shading starting from 15 mm, thus precipitation values between 1–15 mm are not shown), with very high values affecting Northwest Italy. Over this region, the observed precipitation and the 48-hour forecast show values between 30–60 mm, with a small area with values between 60–120 mm. Note, however, that care must be taken when comparing these with single, grid-point observations, since these two fields are defined on a 0.25° grid, and thus represent average values at this scale.

Hereafter, attention will focus on the probabilistic prediction of 48-hour accumulated precipitation exceeding these two values: 15 and 30 mm.

Figure 5 shows the EPS probabilistic forecasts of 48-hour accumulated precipitation exceeding 15 and 30 mm issued on the 25th (T+48 to T+96 hour) and 23rd (T+96 to T+144 hour). The corresponding forecasts issued on the 21st (T+144 to T+192 hour) and 19th (T+192 to T+240 hour) of April are given in Figure 6.

The EPS forecasts issued on the 23rd (Figure 5a) give probabilities of 40%–100% of precipitation exceeding both thresholds in the area where these amounts were observed. The probabilities issued two days earlier, on the 23rd (Figure 5b), are still correctly located and

similar to those for the 15 mm threshold, but lower for the 30 mm threshold.

Forecast probabilities issued four days earlier, on the 21st (Figure 6a), are also correctly positioned for the 15 mm threshold, although they are now lower, 20%–40%, while the probabilities for the 30 mm threshold are positioned to the west of the area where this amount of rain was observed. This is an indication of a too slow propagation of the trough in the EPS forecasts. The forecast probabilities issued on the 19th (Figure 6b) give a 10%–20% probability that precipitation in excess of 15 mm could affect the Po' Valley, and signal that there is a 2–10% probability that precipitation could exceed 30 mm.

Although it is not possible to judge the quality of the EPS probabilistic precipitation forecasts from one case only (for this we refer the reader to published literature, see e.g. *Pappenberger & Buizza (2008)* and *Bartholmes et al. (2009)*), these maps indicate that the EPS gave good probabilistic forecasts up to T+192 hour, with a weaker signal also present at T+240 hour.

Flood forecasts

EFAS gave the first indications of a possible flooding in the Po' river basin in the forecast issued at 12 UTC

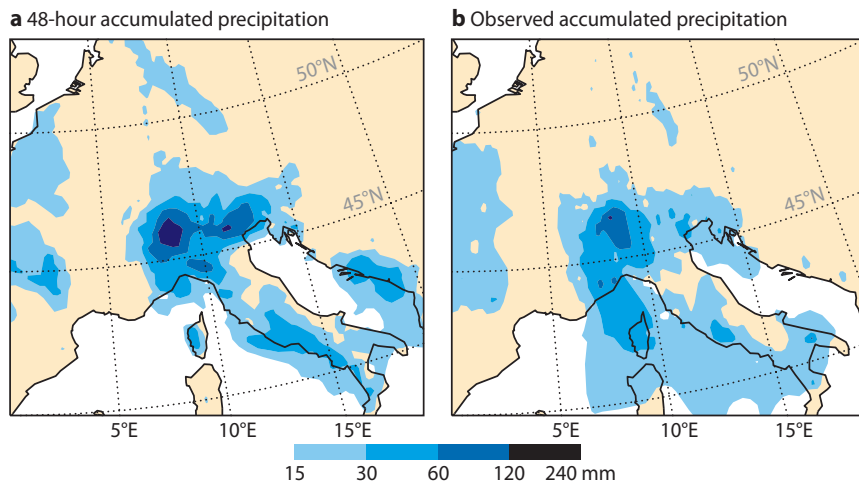


Figure 4 (a) The 0-48 hour forecast of accumulated precipitation in excess of 15 mm from the ECMWF high-resolution model (T799L91) issued at 12 UTC on 27 April and valid between 12 UTC on the 27th and 29th. (b) The 48-hour accumulated observed precipitation, computed by interpolating onto a regular grid the observations from SYNOP stations. The shading indicates the precipitation intervals specified in the legend.

on 21 April. However, the number of ECMWF EPS members (and also of the single forecasts from the DWD and ECMWF high-resolution systems) exceeding alert thresholds were not persistent until the 00 UTC forecast from the 24th. On that date, both single high-resolution forecasts and the probabilistic forecasts simulated discharges exceeding the EFAS high-level threshold throughout the Po' catchment, and confirmed the earlier indications of a possible flooding from the previous forecasts. Hence, a flood alert was sent on the 24th to the Italian national authorities, informing them about the high risk of flooding in the Po' basin from

27 April until 2 May. The alert suggested that they should keep on monitoring the situation carefully using the subsequent forecasts on the EFAS web interface as well as on their national systems.

Figure 7 shows the spatial distribution of the number of ensemble members of the ECMWF EPS forecast (started at 00 UTC on 24 April) simulating discharges which exceed the high-level threshold. EFAS predicted increased, though not extreme, discharges for almost all tributaries within the Po' catchment. The increased flows were principally caused by the predicted heavy precipitation and only to a minor extent by snowmelt

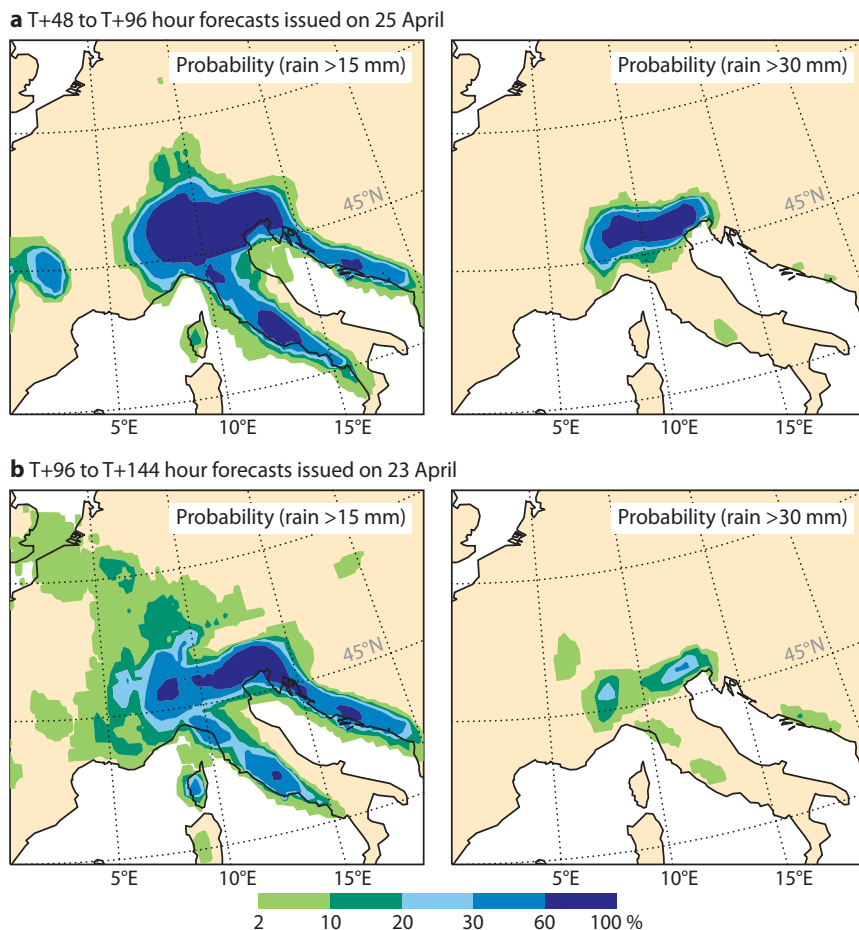
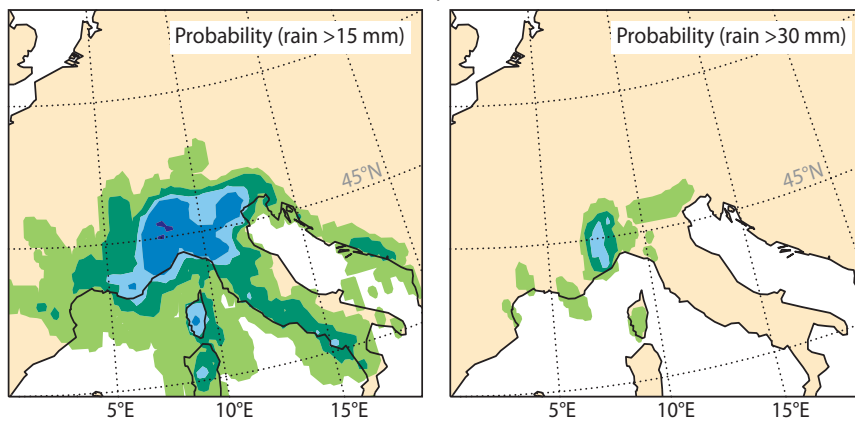


Figure 5 (a) T+48 to T+96 hour forecast probability of occurrence of precipitation in excess of 15 mm (left) and 30 mm (right) issued on 25 April. (b) The corresponding T+96 to T+144 hour forecast probability issued on 23 April. The shading indicates the probability intervals specified in the legend.

a T+144 to T+192 hour forecasts issued on 21 April



b T+192 to T+240 hour forecasts issued on 19 April

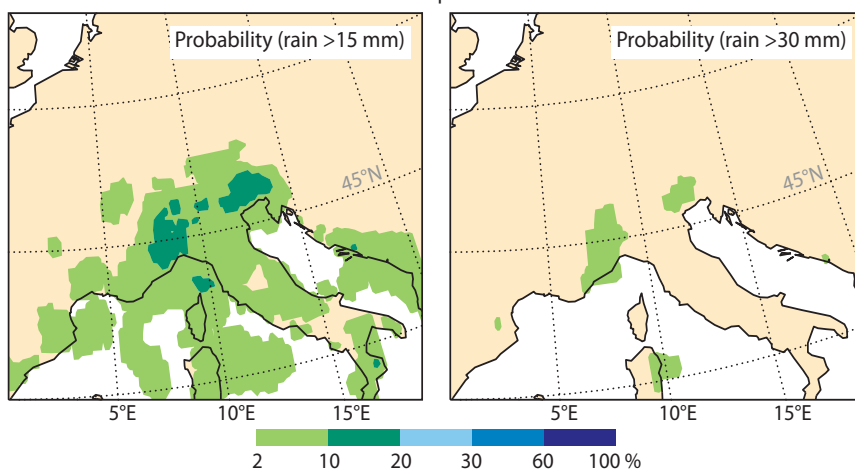


Figure 6 (a) The T+144 to T+192 hour forecast probability of occurrence of precipitation in excess of 15 mm (left) and 30 mm (right) issued on the 21 April. (b) The corresponding T+192 to T+ 240 hour forecast probability issued on 19 April. The shading indicates the probability intervals specified in the legend.

processes, despite the exceptionally large snow accumulations in the Southern Alps. However, the increase in discharge for the majority of tributaries resulted in significantly high flows in the main part of the Po’.

The temporal development of the EFAS/EPs forecasts for reporting points close to Alessandria (upper Po’), Piacenza (lower Po’) and Ferrara is illustrated in Figure 8.

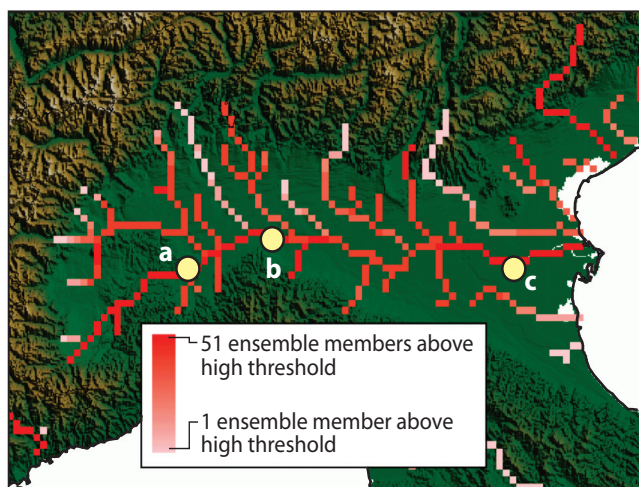


Figure 7 Number of ensemble members based on the ECMWF EPS forecast from 00 UTC on 24 April simulating discharges which exceed the EFAS high alert level for the Po river basin. The circles denote the locations of reporting points as used in Figure 8.

The probabilistic forecast indicated that the highest risk of flooding would occur around 28 and 29 April in the upstream part of the Po’, and around 29 April to 1 May for the downstream part. However, the start of the flooding on the 27th in the upper Po’ and on the 28th in the lower Po’ showed a varying number of ensemble members simulating discharges above the threshold level even with a lead time of two days. This was most likely caused by the temporal resolution of the EFAS simulations and/or the different initial conditions.

Figure 9 illustrates the added value of using probabilistic forecasts. Neither of the EFAS forecasts driven by the single, high-resolution forecasts (ECMWF T799L91 and DWD) could capture the likely high increase of discharge from the 27th onwards. Although both single forecasts lie within the uncertainty range predicted by the probabilistic forecasts, it was not until the 00 UTC forecast on the 26th that a significant exceedance of the alert level was predicted (not shown here).

Unfortunately, no discharge values are yet available for the location shown in Figure 9. Nevertheless, the observed water levels at a reporting station close to Alessandria (Figure 10) confirm the predicted peak on the 28th, although the EFAS forecasts simulate a longer-lasting exceedance of high alert levels. Note that alert levels between EFAS and national/local authorities cannot be compared directly as they were derived

a Alessandria

Forecast day	22	23	24	25	26	27	28	29	30	01	02	03	04
2009042200					2	21	22	16	11	4			
2009042212					34	38	35	30	22	13			
2009042300						44	47	46	38	30	24		
2009042312					45	48	48	46	40	33	24		
2009042400					8	44	46	45	45	40	32	25	
2009042412					31	40	38	36	31	21	16	15	
2009042500					6	29	31	23	21	10	6	4	3
2009042512					42	45	40	37	34	25	21	15	9

b Piacenza

Forecast day	22	23	24	25	26	27	28	29	30	01	02	03	04
2009042200							19	18	4	1			
2009042212						21	32	21	10	3			
2009042300						4	38	43	27	10			
2009042312						44	48	42	22	6	3		
2009042400						23	44	46	43	23	1	1	
2009042412						36	41	39	28	6	2	5	
2009042500						8	43	40	25	4			
2009042512						44	47	42	34	7	2		

c Ferrara

Forecast day	23	24	25	26	27	28	29	30	01	02	03	04	05
2009042200							20	26	28	20			
2009042212						17	37	40	37	18			
2009042300						13	43	46	40	29			
2009042312						35	42	44	40	31	11		
2009042400						31	46	45	44	35	14		
2009042412						51	51	51	49	41	20	4	
2009042500						3	47	51	51	51	42	15	3
2009042512						40	51	51	51	49	29		

Figure 8 Temporal evolution of the ECMWF EPS ensemble members exceeding the EFAS high alert level for a location close to (a) Alessandria, (b) Piacenza and (c) Ferrara. The column on the left denotes the date and time of the forecast. The colour scale indicates the number of ensemble members above the high alert level (see also Figure 7), and can be used to compute the probability of occurrence of high-alert conditions.

differently. Overall, the comparison of the forecasts with observations at other locations reported by ARPA-SIM after the flooding occurred indicated that EFAS predicted the high risk of flooding with a lead time of three to four days.

EPS/EFAS future changes

One of the key advantages of ensemble prediction systems compared to systems that rely on one single forecast is that they can be used not only to identify the most likely outcome, but also to assess the probability of occurrence of extreme/rare events. The EPS/EFAS discharge prediction for Alessandria illustrated that this was actually the case for the situation that occurred on 28–30 April.

Work is progressing to continuously improve the ECMWF EPS and the JRC EFAS systems.

It is planned that ECMWF will introduce three key modifications to the EPS that are expected to further improve its quality.

- ◆ The scheme used to simulate the effect of model errors is going to be upgraded.
- ◆ The methodology followed to generate the EPS initial conditions is going to be modified to include an ensemble data assimilation system.
- ◆ The EPS resolution during the first 10 days will be increased from 50 to about 30 km. In parallel to this change the resolution of the single high-resolution and of the data-assimilation system will also be increased.

These changes are expected to further improve the quality of EPS probabilistic forecast. Results from this work will be reported in due course.

In the near future EFAS is expected to improve its performance significantly through the assimilation of data from higher-density station networks, which are now collected in real time through the EU-FLOOD-GIS data collection system running at the JRC. This will improve the calibration of the system, the determination of critical thresholds and the calculation of initial conditions.

While case studies will remain an important part of the verification of the skill of the system to predict medium to major floods, a newly developed skill score module is now being implemented pre-operationally to monitor the skill of the probabilistic forecasts at regular intervals. In addition to the constant improvement of EFAS as an early flood warning system in Europe, it is also investigating which other products from EFAS could be made available to the partners and researchers in general (e.g. European soil moisture maps, low flow calculations or flood monitoring).

Furthermore, feasibility studies are currently ongoing to test if EFAS methodologies can be transferred to African basins, where climatology is different than in mid-latitude Europe, and where an early warning system needs to satisfy different requirements. If successful, an extension to a global application could be envisaged.

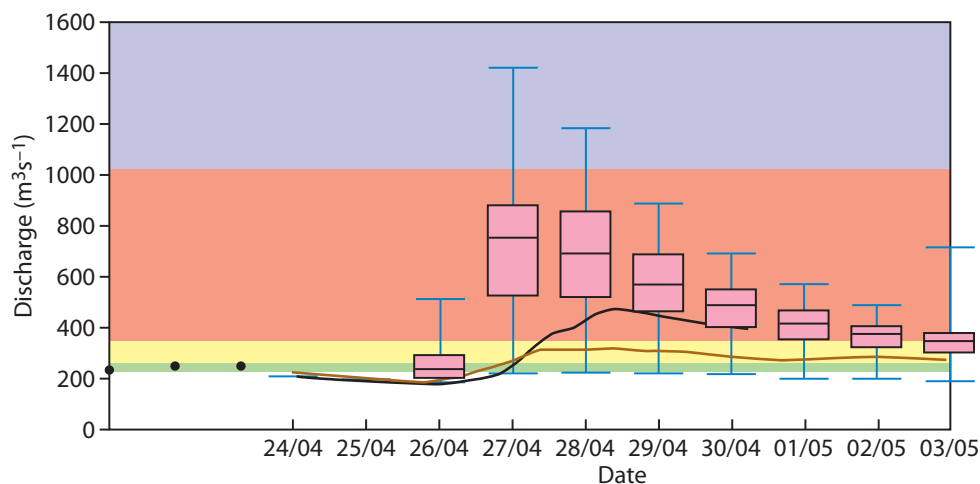


Figure 9 Hydrograph for the reporting point close to Alessandria (see also top panel of Figure 7) for the 00 UTC forecast on the 24 April. The black dots denote the discharge as simulated based on observed data. The black and brown solid lines denote the predicted discharge using the single high-resolution forecasts from the DWD and ECMWF, respectively. Note that the DWD forecast ends at T + 168 hour. The Box-Whisker plots denote the predicted discharges using the ECMWF EPS forecasts. The background colours correspond to the low (green), medium (yellow), high (red) and severe (purple) alert levels.

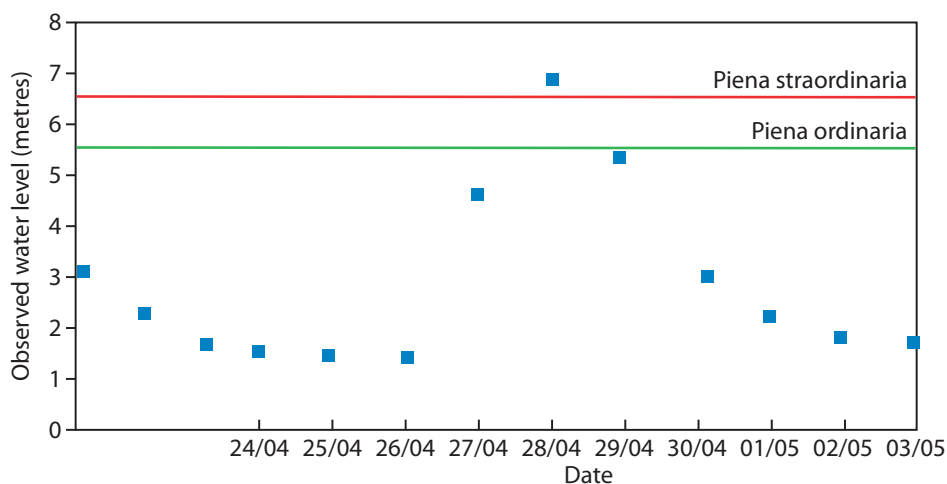


Figure 10 Daily averaged observed water levels at a reporting point close to Alessandria. Green and red solid lines denote the ordinary and extraordinary alert levels (piena ordinaria and piena straordinaria) as used by the Piemonte regional authorities.

FURTHER READING

Bartholmes, J.C., J. Thielen, M.H. Ramos & S. Gentilini, 2009: The European Flood Alert System EFAS – Part 2: Statistical skill assessment of probabilistic and deterministic operational forecasts. *Hydrol. Earth Syst. Sci.*, **13**, 141–153.

Buizza, R., Y.-Y. Park, M. Leutbecher & F. Pappenberger, 2008: Predictability studies using TIGGE data. *ECMWF Newsletter No. 116*, 16–20.

Buizza, R., J.-R. Bidlot, N. Wedi, M. Fuentes, M. Hamrud, G. Holt, T. Palmer & F. Vitart, 2006: The ECMWF Variable Resolution Ensemble Prediction System (VAREPS). *ECMWF Newsletter No 108*, 14–20.

Palmer, T.N., R. Buizza, M. Leutbecher, R. Hagedorn, T. Jung, M. Rodwell, F. Vitart, J. Berner, E. Hagel, A. Lawrence, F. Pappenberger, Y.-Y. Park, L. van Bremen & I. Gilmour, 2007: The ECMWF Ensemble Prediction System: recent and on-going developments. A paper presented at the 36th Session of the ECMWF Scientific

Advisory Committee. *ECMWF Tech. Memo. No 540*.

Pappenberger, F. & R. Buizza, 2008: The skill of ECMWF precipitation and temperature predictions in the Danube basin as forcings of hydrological models. *ECMWF Tech. Memo. No. 558*.

Thielen, J., J. Schaake, R. Hartman & R. Buizza, 2008: Aims, Challenges and Progress of the Hydrological Ensemble Prediction Experiment (HEPEX): a summary of the 3rd HEPEX workshop held in Stresa 27–29 June 2007. *Atmos. Sci. Lett.*, **9**, 29–35.

Thielen J., J. Bartholmes, M.-H. Ramos & A. de Roo, 2009: The European Flood Alert System-Part 1: Concept and development. *Hydro. Earth Syst. Sci.*, **13**, 125–140.

Vitart, F., A. Bonet, M. Balmaseda, G. Balsamo, J.-F. Bidlot, R. Buizza, M. Fuentes, A. Hofstadler, F. Molteni & T.N. Palmer, 2008: Merging VAREPS with the monthly forecasting system: a first step towards seamless prediction. *ECMWF Newsletter No. 115*, 35–44.

NEMOVAR: A variational data assimilation system for the NEMO ocean model

KRISTIAN S. MOGENSEN,
MAGDALENA ALONSO BALMASEDA, ANTHONY WEAVER,
MATTHEW MARTIN, ARTHUR VIDARD

THE OCEAN-ATMOSPHERE coupled model used for monthly and seasonal forecasts requires the modelling and initialization of the three-dimensional global ocean. To this end, ECMWF has been using the HOPE (Hamburg Ocean Primitive Equation) ocean model and an Optimal Interpolation (OI) data assimilation system since the beginning of the coupled-model forecasting activities in 1995. However, with the consolidation of a large part of the European ocean modelling activities around NEMO (Nucleus for European Modelling of the Ocean; *Madec*, 2008), it was decided that ECMWF should adopt NEMO as the ocean component of its coupled forecasting system.

NEMO is a comprehensive ocean modelling framework consisting of a dynamical ocean model (OPA), sea ice model (LIM) and biochemistry models. ECMWF is primarily concerned with the ocean component of the NEMO system, but is planning to investigate the use of the LIM sea ice model in the future. The next operational seasonal forecast system (System 4) will use the atmospheric model from the Integrated Forecast System (IFS) linked to NEMO via the OASIS coupler that is used to exchange relevant fields. The same coupled models will also be used for monthly forecasting within the ECMWF Ensemble Prediction System (EPS).

Part of the transition from HOPE to NEMO involves setting up a new system for providing ocean initial conditions. Rather than adopting the current OI scheme used by HOPE, it was decided to pursue the development of a variational-based assimilation system (NEMOVAR) in collaboration with CERFACS (European Centre for Research and Advanced Training in Scientific Computation) and the Met Office. Other research institutes, such as INRIA/LJK (Institut National de Recherche en Informatique et Automatique/Laboratoire Jean Kuntzmann) based in Grenoble, are also making significant contributions to NEMOVAR. Though we usually refer to this system as NEMOVAR, at present it only applies to the dynamical ocean part

(OPA) of the NEMO system. This article describes the implementation plan and current status of NEMOVAR.

Development of NEMOVAR

The basis for the NEMOVAR developments is OPAVAR (*Weaver et al.*, 2005), a variational assimilation system developed for a previous version of OPA. The OPAVAR system has been used for several studies as well as European research projects such as DEMETER, ENACT and ENSEMBLES. It supports 4D-Var as well as 3D-Var since it includes the tangent-linear and adjoint codes of the previous version of OPA. It has mostly been used for low-resolution ($\sim 2^\circ$) studies of the global ocean. It is based on an incremental algorithm with outer and inner ‘loops’, similar to that of the IFS 4D-Var. These concepts will be discussed later.

OPAVAR has three major drawbacks.

- ◆ It is based on an obsolete version of OPA that is no longer maintained as part of NEMO.
- ◆ It is not straightforward to adapt to different ocean model resolutions.
- ◆ It cannot be run using distributed memory parallelization.

These points are severe limitations when porting the code to future computer architectures and for higher resolution applications.

For these reasons it was decided to develop NEMOVAR. In the following we summarize the key features of OPAVAR and describe the implementation of NEMOVAR.

The OPAVAR legacy

OPAVAR is able to assimilate observations from subsurface profiles of temperature and salinity, along-track sea level anomaly (SLA) observations from satellite altimeters, and sea surface temperature (SST) maps. It has a multivariate background-error formulation for temperature, salinity, horizontal components of velocity, and sea surface height. The multivariate formulation captures the local relationship between temperature and salinity obtained by imposing approximate preservation of water masses, an equation of state relating temperature and salinity to density, geostrophic adjustment of the horizontal components of velocity, and local relationships between sea surface height and vertical density profiles. The details can be found in *Weaver et al.* (2005) and references therein.

Like most assimilation systems, OPAVAR uses a mechanism where observations within a given time window are collected to compute an analysis. The analysis is obtained by combining observations with a first-guess

AFFILIATIONS

Kristian S. Mogensen, Magdalena Alonso Balmaseda,

ECMWF, Reading, UK

Anthony Weaver, CERFACS, Toulouse, France

Matthew Martin, Met Office, Exeter, UK

Arthur Vidard, INRIA/LJK, Grenoble, France

(background) field, i.e. the previous analysis propagated to the current analysis time using the model. The details are given in Box A.

Development of the current version of NEMOVAR

For the development of NEMOVAR the following tasks were identified:

- ◆ Development of observation operators.
- ◆ Development of an assimilation system that is based on 3D-Var.
- ◆ Implementation of an online, automatic system for the quality control of real-time observations.
- ◆ Development of a system to produce an ensemble of analyses to provide estimates of the uncertainty in the ocean initial conditions.
- ◆ Development of the tangent-linear and adjoint models of the ocean component of NEMO.
- ◆ Development of an assimilation system that is based on 4D-Var.

The first four tasks are needed for the initial operational implementation of NEMOVAR at ECMWF, which in addition will require other developments (see later). Some of the tasks are not completely independent. The 3D-Var system needs the observation operators in order to compute the cost function to be minimized. However, other components such as the quality control

of observations and the NEMO tangent-linear and adjoint models are independent and allow for parallel developments by different groups.

The observation operators in NEMO are central to NEMOVAR but are also valuable for model validation since they allow online comparison with a variety of datasets. Presently, observation operators have been developed for temperature and salinity profiles, SLA from satellite altimeters, SST (both from maps and from individual measurements), and currents (e.g. from the TAO (Tropical Atmosphere Ocean) dataset). The observation operator for currents is a new development that is not available in OPAVAR.

The NEMOVAR 3D-Var system has reached a fairly mature state. The first assimilation experiments for extended periods have been performed by assimilating temperature and salinity data from the quality controlled EN3 dataset provided by the Met Office as part of ENSEMBLES (an EU-funded project that aims to construct scenarios of future climate change with ensemble simulations of Earth-system models). This new dataset includes corrections to expendable bathythermographs (XBTs) to compensate for errors in their fall-rates. Some of the results from these experiments will be discussed below.

Work is ongoing to improve the specification of the observation-error and background-error covariances and the models used to represent them in NEMOVAR. In addition, work is being carried out to implement a multivariate model bias correction scheme similar to the one that exists in the current HOPE/OI (System 3). The basic modules for assimilation of SLA and SST data are in place, and testing is underway.

The work on the tangent-linear and adjoint of the NEMO model is in an advanced state and development of a prototype 4D-Var system will start later this year.

The quality control system used by the Met Office (*Ingleby & Huddleston, 2007*) for their operational ocean forecasting system and for producing the ENSEMBLES datasets has been implemented in the NEMOVAR system. The system is currently used for temperature and salinity profiles and will be extended to include SLA and SST data.

Results from some preliminary experiments will now be described.

Setup of the experiments

The next ECMWF seasonal forecasting system, based on NEMO, will use a 1° global configuration. This configuration, known as ORCA1, has been chosen for the initial experimentation with NEMOVAR.

The impact of assimilation is assessed by comparing a 3D-Var experiment with an experiment without data assimilation (the control). Both experiments are forced with daily atmospheric data from the ERA-Interim reanalysis. They start with the same initial conditions, obtained after 20 years of spin-up using daily climatological data from ERA-Interim. The model SST is

Box A

Variational algorithm implemented in OPAVAR and NEMOVAR

The variational algorithm implemented in OPAVAR, which has been migrated to NEMOVAR, consists of the following steps:

- ◆ An initialization phase which computes the initial (background) model trajectory and the misfits between the observations and this trajectory. This model integration uses the model state at the end of the previous cycle as the starting point.
- ◆ One or several outer loops consisting of:
 - An inner loop that minimizes a quadratic cost function to produce a set of increments (changes to the model field). This cost function depends on the trajectory and the misfits.
 - An update of the trajectory and misfits, obtained by applying the increments to the model. The updated misfits and trajectory can then be used as input for another minimization if multiple outer loops are required.

The analysis is formed by adding the resulting increments to the first guess. This can be performed either directly or by using Incremental Analysis Updates (IAU) where the increments are applied gradually over several time steps. The IAU approach is typically used in 3D-Var to reduce spurious high-frequency adjustment processes resulting from the initialization procedure.

strongly relaxed to external SST analyses (NOAA SST OIv2), and there is a three-year time-scale damping to the climatology of temperature and salinity from the World Ocean Atlas. Rather than using the NEMO ice model, these experiments prescribe the ice cover. The experiments start from an initial state on January 1989 and continue until the end of 2006.

For the control experiment, the model equivalent of the temperature and salinity observations were computed for diagnostic purposes only, whereas for the 3D-Var experiment both the temperature and salinity data were assimilated. An assimilation window of 10 days was used. The 3D-Var experiment was performed with a single outer loop and a fixed set of 40 iterations used for minimization in the inner loop. With the settings used for this experiment the computational cost of the inner loop is roughly equivalent to a 10-day model integration. This means that two thirds of the computer time is spent on integrating the model for the 3D-Var system since two model integrations are needed: one for the background trajectory initialization and one for the application of the analysis increment. For different configurations this cost ratio might change.

Statistics of the model fit to the observations

Figure 1 shows the root-mean-square (rms) error and mean error (or bias) of the model for (a) potential temperature and (b) salinity observations as a function of depth for the global ocean and for a region in the central Equatorial Pacific (NINO3.4: 5°S–5°N, 170°–120°W). Shown are the values for the control experiment and for both the outer and inner loops of the 3D-Var experiment. The biases and rms errors for the 3D-Var experiment are clearly reduced compared to the control experiment.

The bias between the analysis and the observations in the inner loop is very close to zero at all depths. The outer loop results indicate the fit between the model background and observations in the assimilation window before the analysis is performed. If either the model background or observations are biased, the bias in the outer loop will not be zero – this is clearly the case from Figure 1. As expected the rms error of the inner loop departures is lower than that of the outer loop since we are fitting the observations in the analysis. A large discrepancy between the outer and inner loop fits to the observations is an indication that the model is having difficulty in retaining the information brought by assimilation. Figure 1 shows that this is the case for the central regional of the Equatorial Pacific.

The rms error and bias statistics only give part of the picture. Figure 2 shows histograms of the temperature and salinity departures (model minus observations) for the global ocean and for the central Equatorial Pacific for the two experiments. The histograms reveal that for the NEMO model (both with and without assimilation) there is a large warm tail compared to the observations at a depth of 98 metres. In the deeper ocean (below

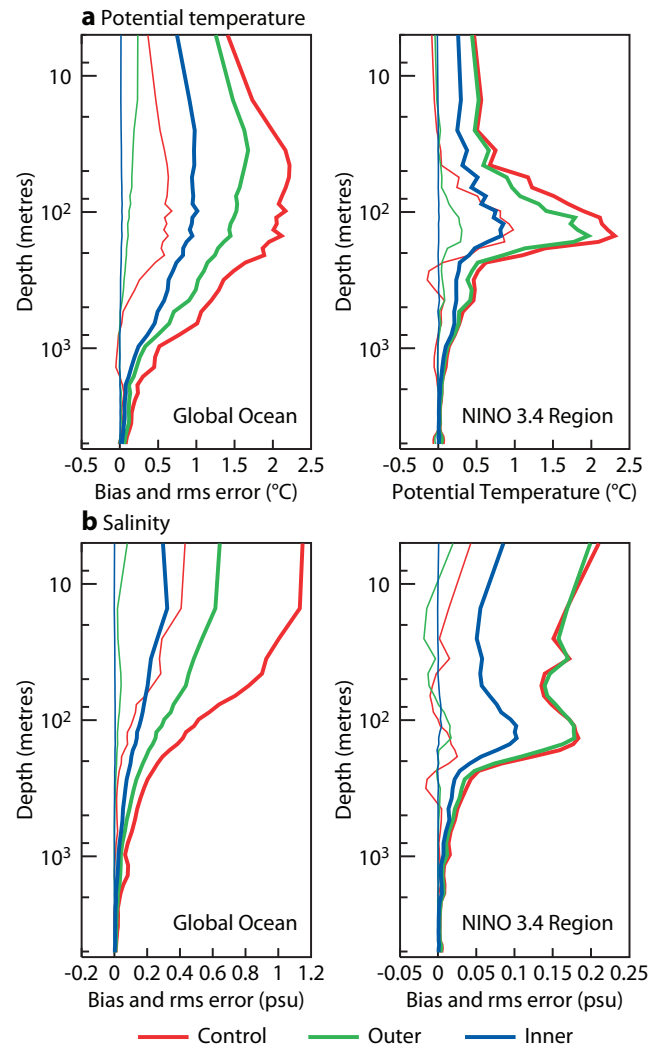


Figure 1 Vertical profiles of the rms error (thick lines) and bias (thin lines) between model and observations for (a) potential temperature (°C) and (b) salinity (practical salinity units, psu) for the global ocean using all observations (left panels) and for observations in the central Equatorial Pacific (NINO3.4) region only (right panels). In the panels, ‘control’ corresponds to the control experiment, ‘outer’ corresponds to the outer loop of the 3D-Var experiment, and ‘inner’ to the inner loop of the 3D-Var experiment. The observations are taken from the EN3 dataset.

approximately 450 metres), there is a large cold tail in the histograms (not shown), indicating that the thermocline in the model is too diffuse. The histograms for the inner loop are very well centred, but in the outer loop a tail towards the warm side develops. Similarly, for salinity the histogram for the outer loop has a distribution that is too salty.

The surface temperature is well constrained by the strong relaxation to the external OIv2 SST analyses. It is found that the biases in salinity are largest at the surface since there is no such constraint on surface salinity. The results also suggest that the assimilation is less effective in the central Equatorial Pacific compared to the global ocean. In the central Equatorial Pacific the rms error of temperature and salinity grows rapidly from the inner loop to the outer loop (i.e. the analysis and forecasts are inconsistent). In the case of salinity,

the information assimilated into the system in a given cycle is lost in the next cycle (see Figure 1b).

Geographical distribution of errors

To investigate the geographical distribution of the errors, the temporal mean of the increments for temperature (Figure 3a) and salinity (Figure 3b) at a depth of 98 metres are considered. These results show several interesting features. The largest increments occur in the area of the western boundary currents and in the tropical ocean (within 10° of the equator). The assimilation tries to compensate for an inaccurate position of the boundary currents which the ocean model, with a resolution of 1°, is unable to represent correctly. Especially noticeable is the dipolar structure of the increments in the Gulf Stream separation area. The assimilation is trying to increase the gradient across the Gulf Stream by adding cool/fresh water to the north of the current and warm/salty water to the south.

In the tropics the story is different. The ocean model has enough resolution to resolve the equatorial dynamics, and therefore the source of model error is likely to

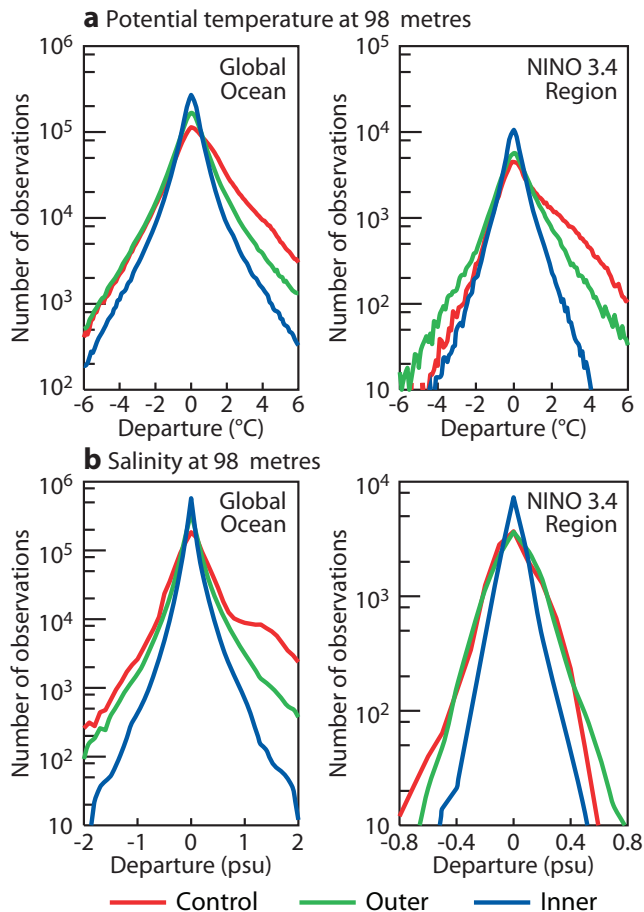


Figure 2 Distribution of model-observation departures at 98 metres depth for (a) potential temperature (°C) and (b) salinity (psu) for the global ocean using all observations (left panels) and for observations in the central Equatorial Pacific (NINO3.4) region only (right panels). In the panels 'control' corresponds to the control run, 'outer' corresponds to the outer loop of the 3D-Var experiment and 'inner' to the inner loop of the 3D-Var experiment. The observations are taken from the EN3 dataset.

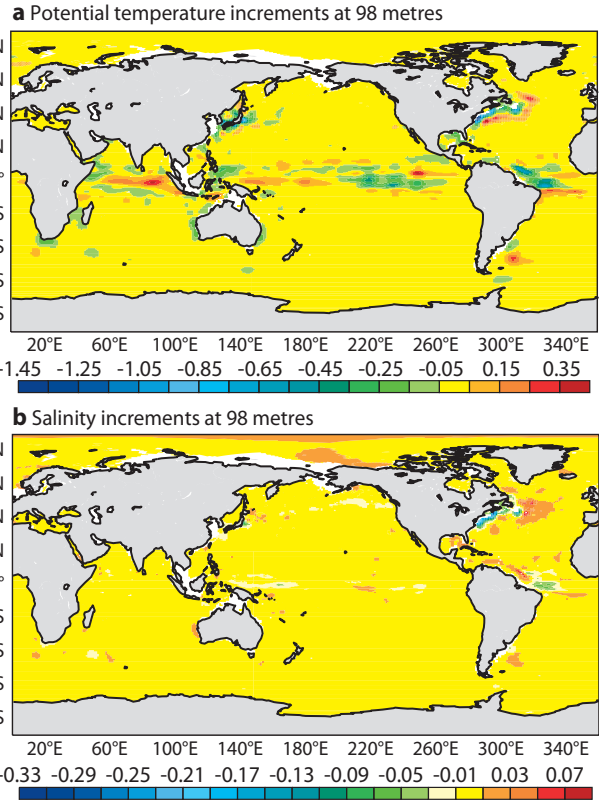


Figure 3 Temporal mean of (a) potential temperature increments (°C) and (b) salinity increments (psu) at 98 metres for all 10-day windows.

reside somewhere else. To investigate this in greater detail, a cross-section of the temperature increments at the equator appears in Figure 4a, together with the temperature differences between the control and assimilation experiments in Figure 4b. In the Pacific the assimilation is trying to steepen the east-west gradient of the thermocline (deepening it in the west and shallowing it in the east). In this experiment, equatorial currents are not improved by assimilating temperature and salinity data (not shown). In the western Pacific they can even be degraded. This aspect should be improved with the introduction of the model bias correction scheme.

The east-west dipolar structure of the assimilation increment contrasts with the mean differences between control and assimilation in Figure 4b, which does not show any east-west dipole: in all the basins, the control experiment is too warm above the thermocline and too cold below it. These results demonstrate that the effect of the assimilation is non-local. How the increments in Figure 4a produce the differences shown in Figure 4b is not obvious. It could be achieved by a variety of processes. For instance, in the Equatorial Atlantic, direct cooling by the assimilation in the western part of the basin, and subsequent advective transport of the negative increments via the equatorial undercurrent, could lead to a basin-wide cooling. Another possible reason is the effect on the vertical mixing: the warm increment in the eastern part of the Indian Ocean around 100 metres (just above the thermocline) could increase the stratification, resulting in reduced vertical mixing of heat down to the

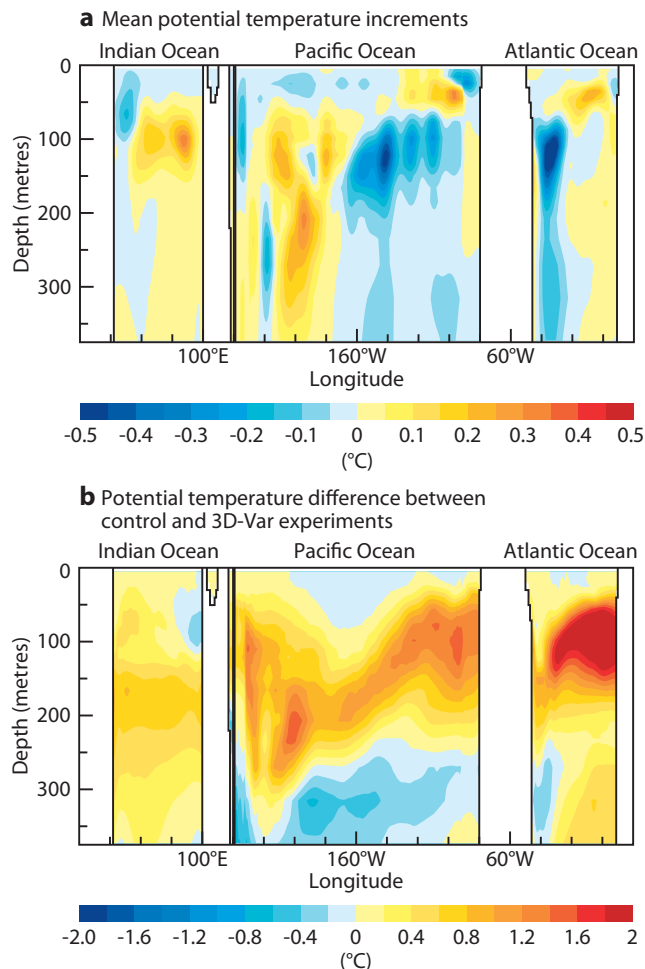


Figure 4 Equatorial cross-section of (a) the temporal mean of all 10-day window potential temperature increments (°C) and (b) the differences in mean potential temperature (°C) between the control and the 3D-Var experiments. The three ocean basins (Indian, Pacific, Atlantic) are illustrated. The averages have been computed for the period of 1989 to 2006. The different spatial structures of the assimilation increment and mean difference demonstrate the non-local effect of the assimilation.

thermocline. A more careful diagnostic study of the different processes involved in the reduction of the error can help to diagnose model errors.

Conclusions and outlook

The preliminary results with the NEMOVAR 3D-Var system are encouraging, but also highlight limitations with the system. Though the assimilation system works correctly according to the assumptions of no model or observation bias, we have demonstrated this is not a valid assumption. The present HOPE OI assimilation system accounts for model bias and the initial results with NEMOVAR seem to indicate that this feature is needed in NEMOVAR as well. Use of information from the assimilation system can be of value in diagnosing model errors and eventually helping to improve the ocean models.

ECMWF plans to use the 3D-Var version of NEMOVAR to produce initial conditions for its coupled ocean-atmosphere modelling system. In the first operational implementation, NEMOVAR will assimilate tempera-

ture, salinity and sea level anomaly data in a global ocean configuration at a 1° resolution (the ORCA1 grid mentioned earlier). A first historical reanalysis based on NEMOVAR for the period 1959 to present will be available to selected users in the autumn of 2009.

Several technical and scientific developments are needed for the operational implementation of NEMOVAR, such as the model bias correction scheme, the real-time quality control of the observations, and the assimilation of altimeter-derived sea level anomalies. The operational implementation of the real-time ocean analyses using NEMOVAR is expected by the spring of 2010.

The Met Office plans to use NEMOVAR for their ocean assimilation activities covering short-range ocean forecasting applications, based on the FOAM (Forecasting Ocean Assimilation Model) system, and seasonal forecasting. The FOAM system runs at two different resolutions including a ¼° global configuration with nested ½° regional configurations. NEMOVAR will be implemented in these systems with a focus on the initialisation of mesoscale eddies, and it is planned to use the upgraded systems in the MyOcean project. This project aims to set up the infrastructures and services in preparation for the GMES (Global Monitoring for Environment and Security) Marine Services.

Several algorithmic improvements and extensions to NEMOVAR are being made at CERFACS and INRIA/LJK. Multi-incremental versions of NEMOVAR are being developed to allow for reduced resolution in the inner loop. This feature will be particularly important for high-resolution applications of 4D-Var. Work is also being done to improve the specified background-error statistics. The long-term development path of NEMOVAR is to a weak-constraint 4D-Var system in which model error is explicitly accounted for in the 4D-Var algorithm.

NEMOVAR will eventually be released under an open source license and made available to a wider community. The precise details for distribution of the NEMOVAR system are currently being discussed.

The development of NEMOVAR has been an effective collaborative international project with many people from various organisations making significant contributions. These developments have also benefited from the support of the NEMO consortium. It is expected that continuing international collaboration will lead to further developments in ocean modelling and data assimilation thereby enhancing the quality of monthly and seasonal forecasts.

FURTHER READING

- Ingleby, B. & M. Huddleston**, 2007: Quality control of ocean temperature and salinity profiles – historical and real-time data. *J. Marine Systems*, **65**, 158–175.
- Madec, G.**, 2008: NEMO ocean engine. *Note du Pôle de Modélisation, Institut Pierre-Simon Laplace (IPSL)*, No 27.
- Weaver, A.T., C. Deltel, E. Machu, S. Ricci & N. Daget**, 2005: A multivariate balance operator for variational ocean data assimilation. *Q. J. R. Meteorol. Soc.*, **131**, 3605–3625.

Improvements in the stratosphere and mesosphere of the IFS

PETER BECHTOLD, ANDREW ORR,
JEAN-JACQUES MORCRETTE, RICHARD ENGELEN,
JOHANNES FLEMMING, MARTA JANISKOVA

IN THE middle atmosphere, which comprises the stratosphere and the mesosphere, the general circulation is driven by the processes of radiation and wave drag due to gravity waves and planetary waves. The term ‘wave drag’ is understood as the deceleration/acceleration of the flow due to breaking waves, as during the dissipation process waves ‘drag’ the flow towards their own horizontal phase speed.

The physics of the middle atmosphere is described in Box A. A key feature of the flow in the middle atmosphere is the formation of a strong westerly jet (referred

to as the polar night jet) in the winter hemisphere with a weaker easterly jet in the summer hemisphere. The speed of these jets is limited by the drag exerted on the horizontal winds by dissipating quasi-stationary planetary waves and gravity waves that originate in the troposphere. The quasi-stationary vertically-propagating planetary waves occur mainly in the northern hemisphere due to their orographic origin. These waves are resolved by the model dynamics. The orographic gravity waves emanating from the model-resolved orography are explicitly represented whereas those linked to the subgrid orography are parametrized.

Non-orographic gravity waves are generated by mechanisms such as deep convection, frontal instabilities, shear zones and thermal contrasts. The term non-orographic implies that these waves are non-stationary

Box A Physics of the middle atmosphere

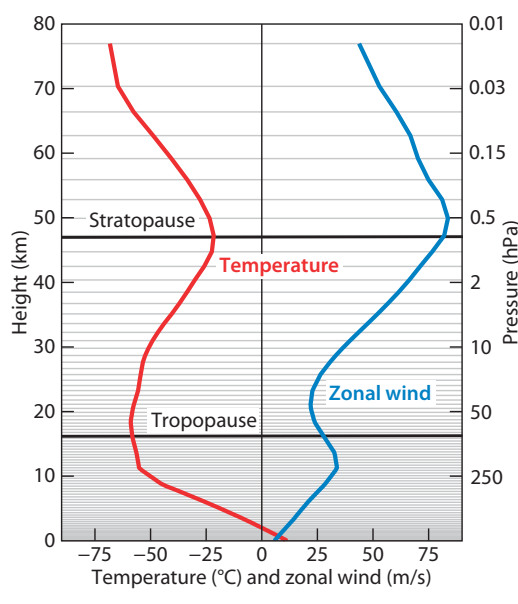
The climatological temperature and wind profiles of the atmosphere for July at latitude 40°S are shown in the figure along with the distribution of the 91 model vertical layers of the IFS.

The temperature decrease with height in the troposphere is due to adiabatic decompression, and the westerly jet in the middle latitudes of the upper-troposphere is generated by the horizontal temperature gradient between the tropical and polar latitudes.

The stratosphere is characterised by an increase in temperature as infrared radiative cooling is offset by heating through the absorption of solar radiation by greenhouse gases, mainly ozone.

Above the stratopause, in the mesosphere, the ozone heating decreases with height, and so does the temperature. The radiative heating has a strong latitudinal variation, with a maximum in the summer polar region and a minimum in the winter polar region. The resulting horizontal temperature gradient between the summer hemisphere and the winter hemisphere creates a meridional circulation, with air rising at the summer pole and sinking at the winter pole. The Coriolis torque acting on the meridional circulation leads in the winter hemisphere to the formation of a strong westerly jet, the so called polar night jet, that peaks at the stratopause at 1 hPa, and can locally attain monthly mean wind speeds of over 100 m s⁻¹ in the southern hemisphere. A weaker easterly jet forms in the summer hemisphere. The only force that can balance the Coriolis torque, and there-

fore limit the horizontal winds, is the drag exerted by dissipating quasi-stationary planetary waves and gravity waves that originate in the troposphere.



Climatological atmospheric temperature and zonal wind profiles for July at latitude 40°S. The thin horizontal lines mark the 91 vertical layers of the IFS. *Troposphere*: extends from roughly 100 hPa (0–15 km) and is represented by 51 model layers. *Stratosphere*: extends from 100 hPa to 1 hPa (15–48 km) and is represented in the IFS by 31 model layers. *Mesosphere*: extends from 1 hPa to 1 Pa (48–80 km) and contains 9 model layers in the current IFS. The top of the mesosphere, the mesopause, corresponds also to the top of the IFS.

(i.e. have non-zero phase speeds). Ground-based and aircraft observations of the waves are available, and recently global data on the wave properties and the associated momentum fluxes have been obtained from infrared radiation measurements onboard satellite by *Ern et al.* (2004) during the CRISTA campaign. It is found that the vertical wavelengths of the waves vary from a few hundred metres to tens of kilometres, and the horizontal wavelengths from tens to thousands of kilometres. Therefore, these waves are generally unresolved or under-resolved by the model and/or their generating mechanism cannot be represented by the model. Consequently, their impact on the middle atmosphere circulation must be parametrized. In this article the implementation of such a parametrization scheme in the ECMWF Integrated Forecast System (IFS) is described.

Parametrization of non-orographic gravity wave drag

Until model cycle Cy35r2 (operational since 10 March 2009) the IFS did not make use of a parametrization scheme for non-orographic gravity wave drag (NOROGWD), but instead above 1 hPa so called Rayleigh friction has been applied – this is a simple deceleration of the flow proportional to the zonal mean wind speed. A parametrization scheme for non-orographic gravity waves has been introduced in Cy35r3 (becoming operational in summer 2009) following the scheme developed by *Scinoccia* (2003) that is itself based on the approach of *Warner & McIntyre* (1996).

The physical principles behind the parametrization scheme are simple and similar to most operational parametrizations. At a certain level in the troposphere a spectrum of waves is emitted in the four main directions (north/south, east/west), having a broad range of vertical wavelengths and frequencies. The launch spectrum is assumed to be independent of time and localisation. For practical reasons computations are performed using horizontal phase speeds instead of frequencies, and the wave package is represented by the total wave momentum flux or Eliassen-Palm flux rather than the total wave energy. The wave package then undergoes conservative vertical propagation until partial dissipation takes place due to two processes:

- ◆ **Critical level filtering.** This occurs when the phase speed of the waves approaches the ambient wind speed. The process requires realistic model winds. It is particularly effective when the wind speed changes sign (e.g. when waves emitted in the tropospheric westerlies meet stratospheric easterly winds).
- ◆ **Non-linear dissipation.** As the amplitude of the waves increases with height due to the decrease in density, the growth of the gravity wave spectrum at large wavenumbers (short waves) is bounded so as not to exceed some ‘saturated’ spectrum.

The scheme requires a few important parameters, namely the shape and amplitude of the wave spectrum at the launch level, the saturation level for the larger

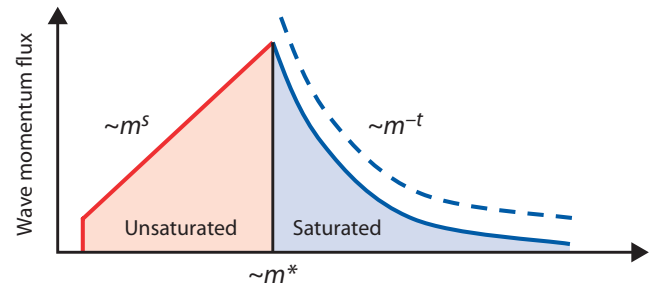


Figure 1 Spectrum of wave momentum flux at the departure level as a function of vertical wavenumber m . The unsaturated and saturated parts are denoted by the red and blue line, respectively, with $s = 1$ and $t = 3$. The characteristic wavenumber m^* typically corresponds to a vertical wave length of 2 km. The dashed line denotes the saturation spectral density. All values are scaled by a fixed amplitude.

vertical wavenumbers, and the launch-level height. The latter is of particular importance as it determines the Doppler shift of the departure wave spectrum by the ambient wind. For the parameter setting we essentially followed *Ern et al.* (2006) who evaluated a version of the Warner and McIntyre scheme against satellite measurements of wave momentum flux during the CRISTA campaign.

The departure level of the waves is set to 450 hPa, and the amplitude of the wave momentum flux is set to a globally constant value of 3.75×10^{-3} Pa. The functional shapes for the unsaturated and saturated part of the spectrum are given in Figure 1, where the characteristic vertical wavenumber m^* separating the two distinctive parts of the spectrum corresponds to a vertical wavelength of 2 km. The unsaturated (long wave) part of the spectrum is naturally less well known as it is difficult to measure. Each time the spectrum exceeds the dashed line in Figure 1 the non-linear dissipation is supposed to occur and the corresponding amount of momentum flux is removed and deposited into the environment. There is one free parameter in the scheme that allows the shifting of the saturation line in Figure 1, and therefore determines the height where non-linear dissipation occurs - this has important consequences for the stratospheric oscillations.

Finally, numerical aspects had to be considered as NOROGWD schemes tend to be computationally expensive with computing times in the range of 15–20% of the total model run time (*Scinoccia*, 2003). For this purpose we reduced the number of spectral intervals to 20 from 50 originally proposed, reduced the calling frequency to 1 or 2 hours (depending on model resolution), and optimised the coding structure. This meant that, without any significant loss of numerical accuracy, the NOROGWD scheme contributes to less than 3% to the total forecast run time.

Trace gas concentrations

The radiative heating/cooling rates of the middle atmosphere strongly depend on the trace gas concentrations. A list of the relevant trace gases, with the exception of

Trace gas	Cy35r2	Cy35r3
CO ₂	536 (353)	584 (384)*
CH ₄	0.953 (1.72)	0.957 (1.73)*
N ₂ O	0.471 (0.31)	0.478 (0.31)
NO ₂	0.794×10^{-4} (0.500×10^{-4})	1.896×10^{-4} (1.194×10^{-4})
CFC ₁₁	1.328×10^{-3} (0.280×10^{-3})	1.169×10^{-3} (0.247×10^{-3})
CFC ₁₂	2.020×10^{-3} (0.484×10^{-3})	2.151×10^{-3} (0.515×10^{-3})

Table 1 Trace gas concentrations in units of $\text{kg kg}^{-1} \times 10^6$, and in parentheses in units of parts per million by volume (ppmV), as used until Cy35r2, and typical annual and atmospheric mean values for Cy35r3 computed from the new climatology that is given as monthly evolving zonal mean fields. Asterisks in Cy35r3 denote values that have been computed from the GEMS reanalysis.

ozone, is given in Table 1. Before Cy35r2 the concentrations for these species have been simply specified as constants following the IPCC/SACC Climate Change 1995 Report (Houghton *et al.*, 1995). The ozone, a quantity that strongly varies with height, has been given by monthly evolving two-dimensional climatological fields as a function of pressure and latitude following Fortuin & Langematz (1994).

The most important greenhouse gases are carbone dioxide (CO₂), ozone (O₃) and methane (CH₄).

Concentrations for these three gases have been replaced in Cy35r3 by new monthly evolving two-dimensional climatologies computed from the GEMS reanalysis that is available so far for the period 2003–2007 (GEMS is an EU-funded project concerned with global and regional Earth system monitoring using satellite and in situ data). For the missing species, such as the nitrogen oxides and the chlorofluorocarbons, we now use two-dimensional climatologies computed from the two-dimensional chemical transport model MOBYDIC by D. Cariolle at Météo-France.

The GEMS derived CO₂ and O₃ climatologies were taken from the year 2006 (when microwave limb sounder data was available O₃) and the CH₄ analysis was taken from the year 2005. These datasets represent the best fit to available observations. Furthermore, the CO₂ and CH₄ climatological fields are trend corrected to account for the man-made increase in greenhouse gas concentrations since 1850.

In order to compare the concentrations in Cy35r3 to the constant values used before Cy35r2, typical global annual mean concentrations have been computed as given in Table 1. One notices the significantly higher CO₂ and CH₄ values in Cy35r3 compared to Cy35r2. Furthermore, as an example, zonal cross-sections of the CO₂ and O₃ mixing ratios for July and January (representative for the year 2006) are illustrated in Figure 2. The CO₂ concentrations vary between 564×10^{-6} and

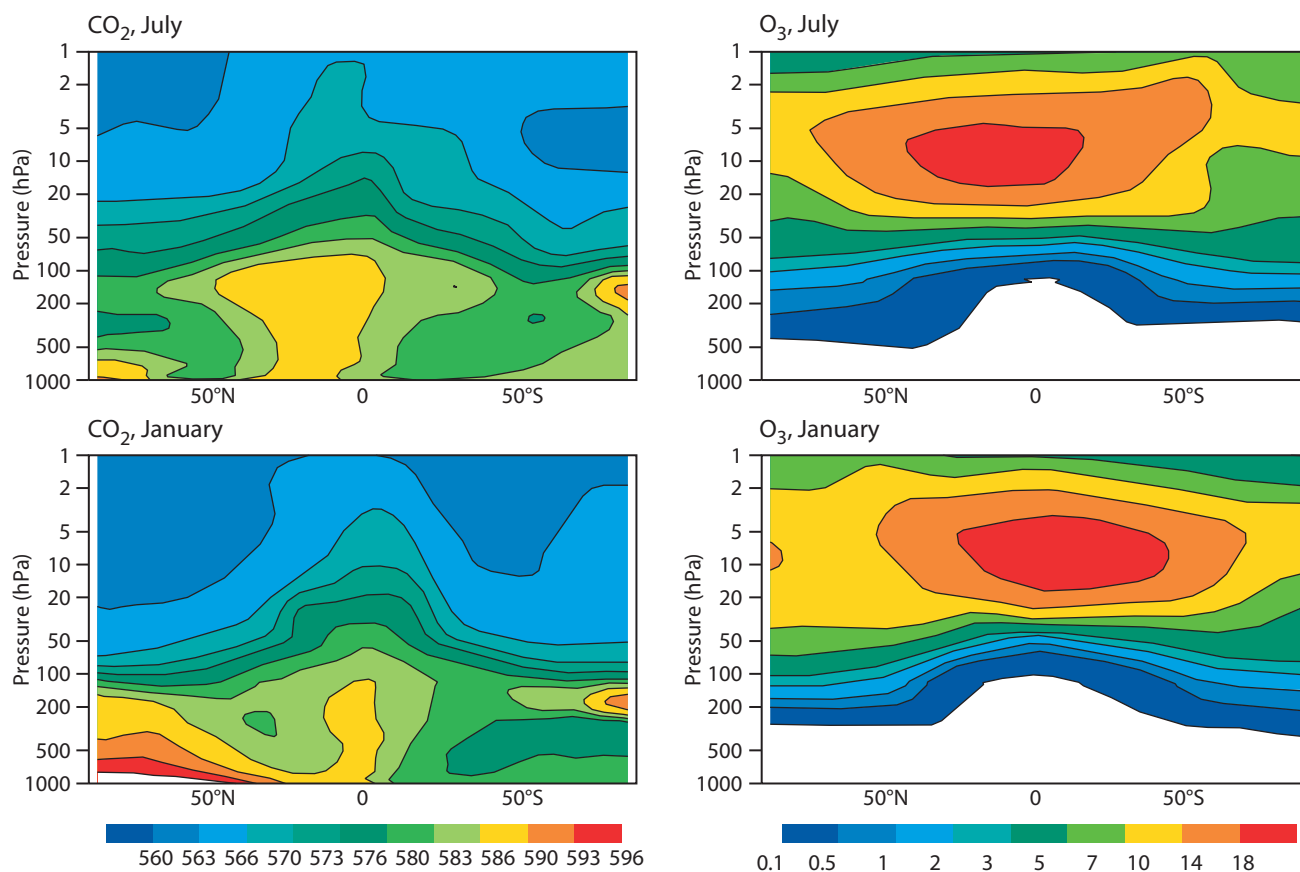


Figure 2 Zonal mean climatological concentrations ($\text{kg kg}^{-1} \times 10^6$) for CO₂ and O₃ from the GEMS reanalysis during July and January.

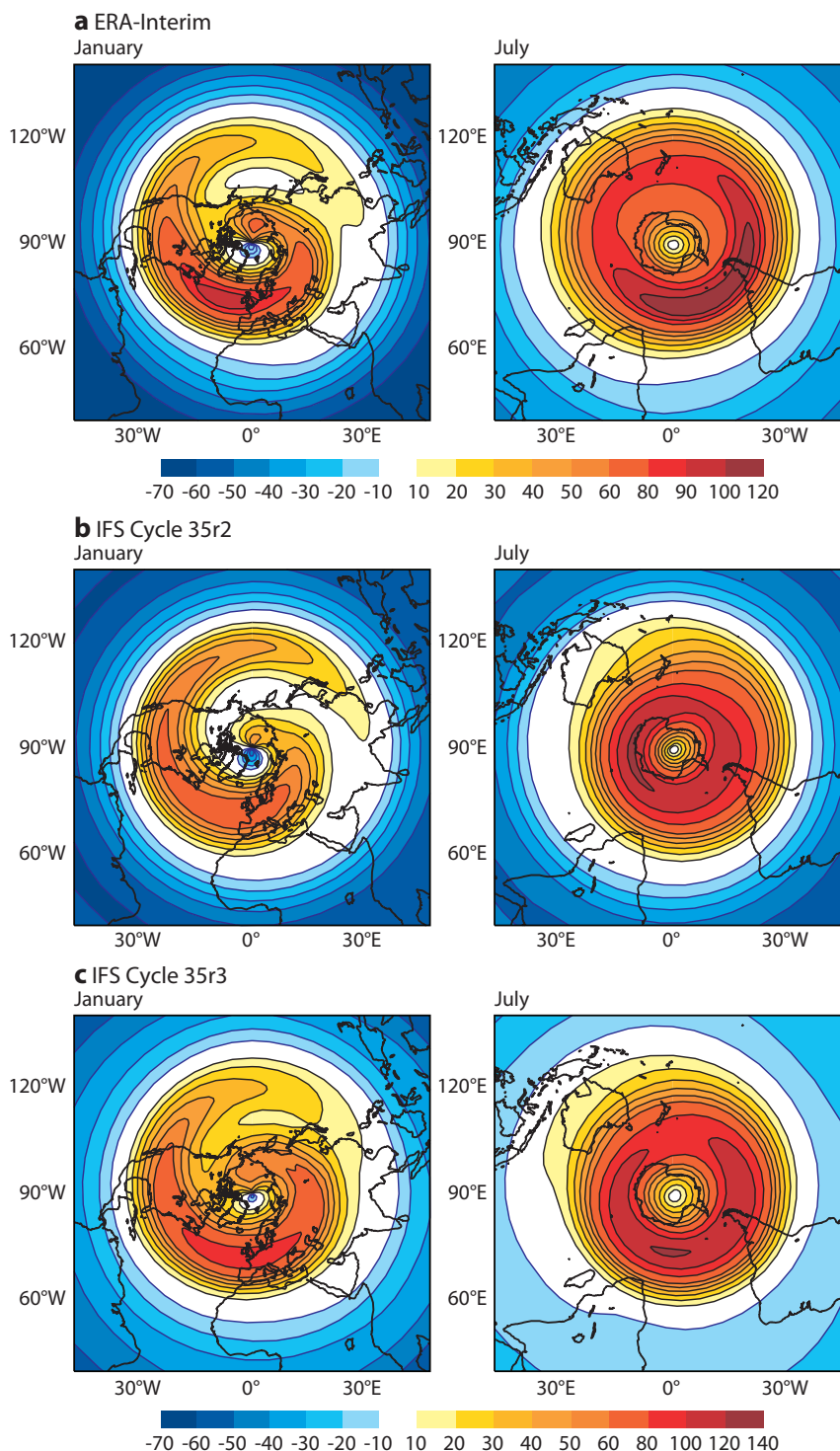


Figure 3 Zonal mean wind speed (ms^{-1}) at 1 hPa for the northern hemisphere polar vortex during January (left column) and the southern hemisphere polar vortex during July (right column) averaged over the period 1993–1998 from (a) the ERA-Interim, (b) Cy35r2, and (c) Cy35r3. The symmetry of the vortex is disrupted in the northern hemisphere by quasi-stationary Rossby waves.

$591 \times 10^{-6} \text{ kg kg}^{-1}$ (371–389 ppmV) with maximum values occurring in the northern hemisphere troposphere. But there is a strong seasonal cycle, and high mixing ratios are also present throughout the tropical troposphere and lower stratosphere due to surface emissions by biomass burning and subsequent vertical convective mixing. In contrast, the O_3 mixing ratios peak in the stratosphere and this leads to strong radiative heating due to the

absorption of solar ultraviolet radiation. Peak concentrations of $18 \times 10^{-6} \text{ kg kg}^{-1}$ (10.86 ppmV) are attained in the tropical upper-stratosphere between 5 and 15 hPa.

Climatology

The SPARC (Stratospheric Processes And their Role in Climate) climatology (www.atmosphysics.utoronto.ca/SPARC/) can be taken as an independent reference

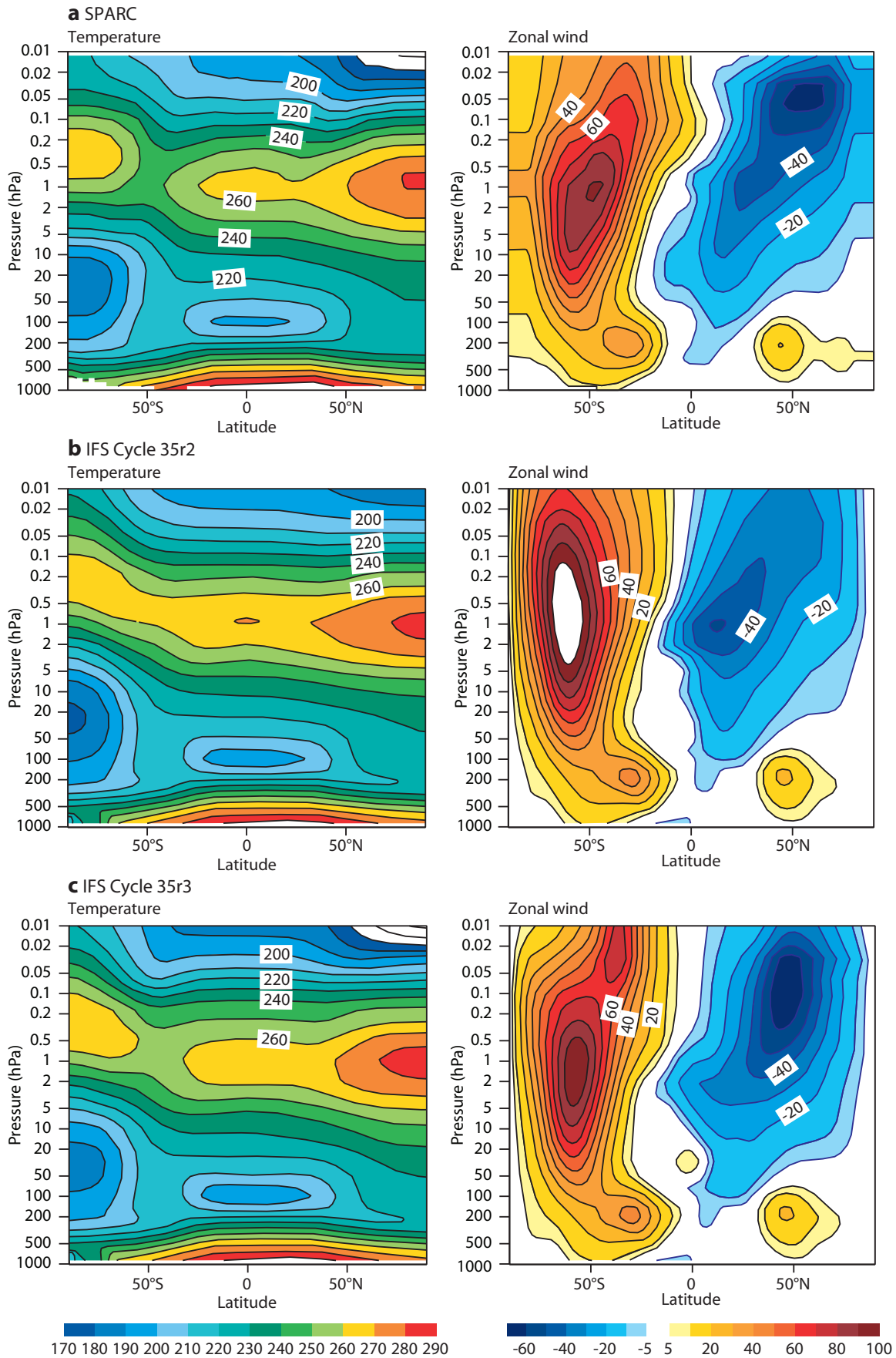


Figure 4 Zonal mean cross-section (latitude versus pressure) of temperature (K, left column) and zonal wind (m s^{-1} , right column) for July from (a) the SPARC climatology, and from an ensemble of one-year T159 integrations for the period 1993–1998 with (b) Cy35r2 and (c) Cy35r3.

dataset for the middle atmosphere, and therefore can be used for model evaluation. Alternatively, one could derive a climatology from the operational ECMWF analysis and reanalysis such as ERA-Interim. However, before Cy35r2, including ERA-Interim, the analysis is not constrained by observations in the mesosphere. Only since Cy35r2, with the introduction of the radiative transfer model RTTOV9, is the operational analysis in the mesosphere weakly constrained by data, mainly from IASI satellite infrared channels onboard MetOp. Furthermore, the ERA-Interim dataset is limited to 0.1 hPa. Therefore, we primarily evaluate the model's middle atmosphere climatology against SPARC, although stratospheric wind data from the ERA-Interim reanalysis will also be considered.

The stratospheric wintertime polar vortex is illustrated in Figure 3 at the 1 hPa level for the northern hemisphere during January (left column) and the southern hemisphere during July (right column). The reanalysis data is compared to the model climatologies of Cy35r2 and Cy35r3 which are obtained for the period 1993–1998 from an ensemble of six one-year forecasts at resolution T159 (125 km) with analysed sea surface temperatures.

ERA-Interim (Figure 3a) shows a quasi-symmetric southern hemispheric polar vortex with maximum monthly mean wind speeds of 120 m s^{-1} . The northern hemispheric polar vortex, by contrast, is weaker and strongly disrupted over the Pacific due to vertically propagating large-scale quasi-stationary Rossby waves.

The ERA-Interim data is reasonably reproduced with model Cy35r2 (Figure 3b). However, the southern hemispheric vortex is too strong and too narrow, and underestimates the local jet maximum between Africa and South America. For the northern hemispheric wintertime vortex, on the contrary, the jet maxima over the North Atlantic are underestimated by up to 20 m s^{-1} , and the wind speeds over the Pacific are overestimated by 10 m s^{-1} .

Cy35r3 (Figure 3c) generally improves the representation of both the northern and southern polar vortex, and is also able to reproduce the local jet maxima. In particular the representation of the jet between Africa and South America during austral winter, as well as the jet over the North Atlantic and Europe during boreal winter, is improved.

Figure 4 shows cross-sections of monthly mean temperature and zonal wind for July from SPARC along with the corresponding model results with Cy35r2 and Cy35r3.

The comparison between SPARC and Cy35r2 for July (Figures 4a and 4b) reveals a 10–20 K warm bias around the stratopause. Also apparent are a 25 K warm bias with Cy35r2 around the northern polar (summer) mesopause and a 10 K cold bias at the southern polar (winter) mid-stratosphere, indicative of an atmosphere with an overturning circulation that is too weak. Furthermore, the south polar wintertime jet is too strong in Cy35r2 and lacks the observed vertical inclination towards the tropics. Also, the mesospheric jet in the northern

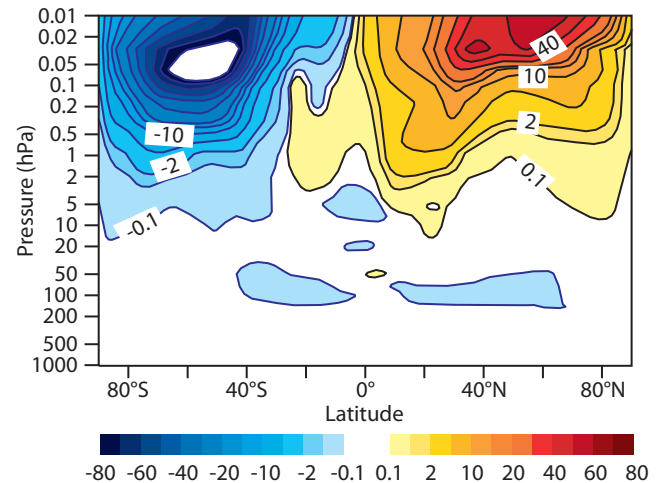


Figure 5 Zonal mean cross-section of the acceleration/deceleration ($\text{m s}^{-1} \text{ day}^{-1}$) of the zonal wind during July due to the NOROGWD.

summer hemisphere is too weak and its core is near the stratopause instead of being located near the mesopause. This bias is directly related to the use of Rayleigh friction formulated in terms of a damping coefficient which increases with height, and which therefore strongly damps any upper-level winds.

In contrast, comparison of SPARC and Cy35r3 (Figures 4a and 4c) shows that Cy35r3 corrects most of the deficiencies of Cy35r2. In particular the temperature structure in the upper stratosphere and mesosphere is improved, and the stratospheric polar winter jet and the mesospheric polar summer jet now present reasonable inclinations with the jet cores at the right height. The reduced temperature errors around the stratopause are due to the improved greenhouse gas climatology, whereas the reduced temperature and wind errors in the mesosphere are a consequence of the strong NOROGWD tendencies in the mesosphere (Figure 5). These decelerate the southern (winter) hemisphere westerly jet with a rate of up to $80 \text{ m s}^{-1} \text{ day}^{-1}$ and also decelerate the northern (summer) hemisphere easterly jet. Overall the results for Cy35r3 represent a significant improvement over previous cycles, but the temperature at the stratopause is still overestimated by 5 K compared to SPARC and the tilt of the polar night westerly jet towards the tropics is underestimated.

A similar picture as for July is obtained for January (Figure 6) but with the wind directions in each hemisphere reversed. Again, Cy35r2 produces a too warm stratopause, a too warm summer polar summer mesopause, and a misplaced core of the summer polar mesospheric jet. The (northern) hemisphere wintertime polar jet is generally much weaker than the southern polar wintertime jet which explains the smaller differences between SPARC and Cy35r2 compared to Figure 4. Again Cy35r3 improves most of the deficiencies of Cy35r2 in the mesosphere and the upper stratosphere. However, the temperature at the stratopause is still too high compared to SPARC and the strength of the polar wintertime jet is overestimated.

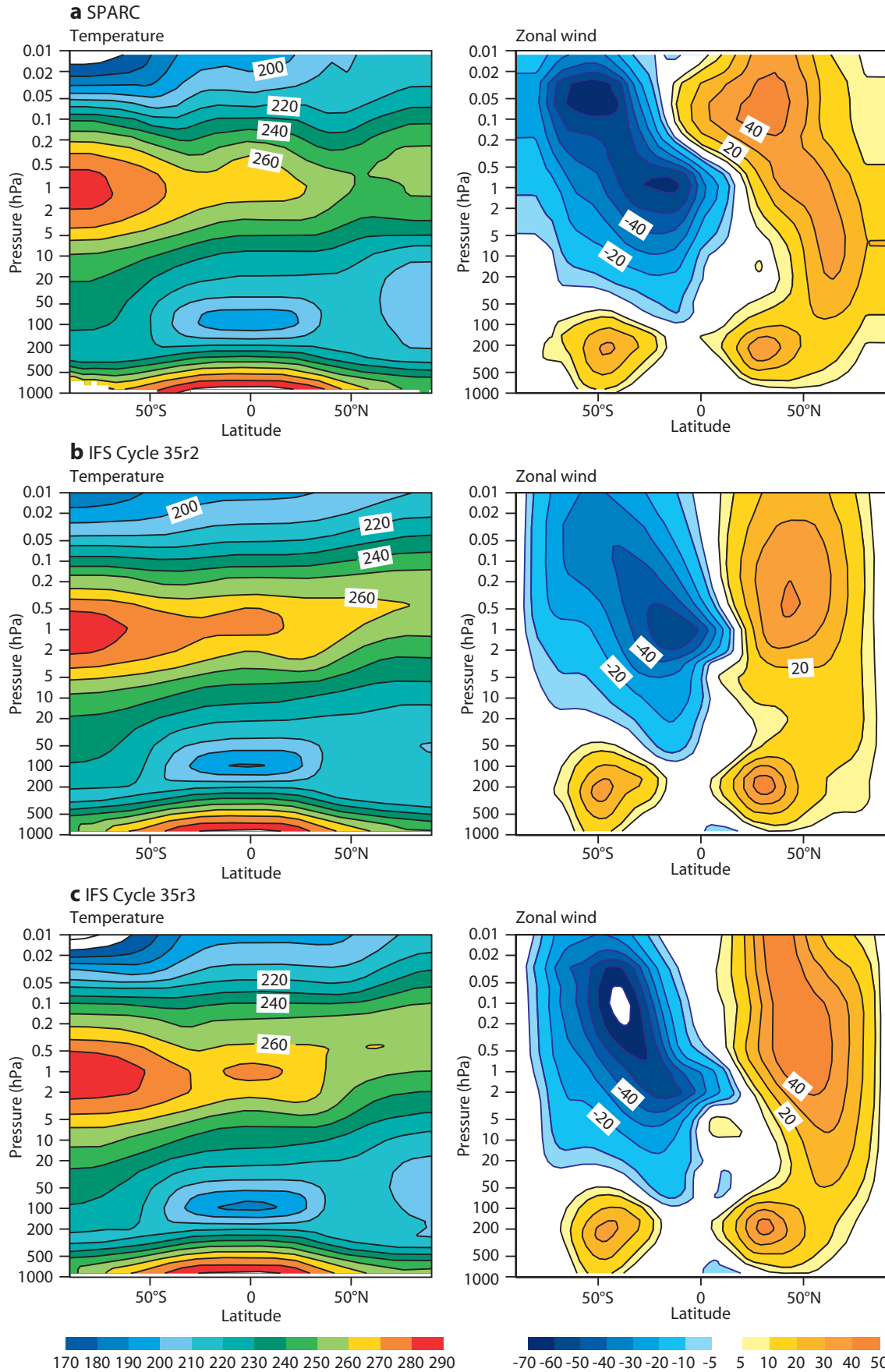


Figure 6 Zonal mean cross-section (latitude versus pressure) of temperature (K, left column) and zonal wind (m s^{-1} , right column) for January from (a) the SPARC climatology, and from an ensemble of one-year T159 integrations for the period 1993–1998 with (b) Cy35r2 and (c) Cy35r3.

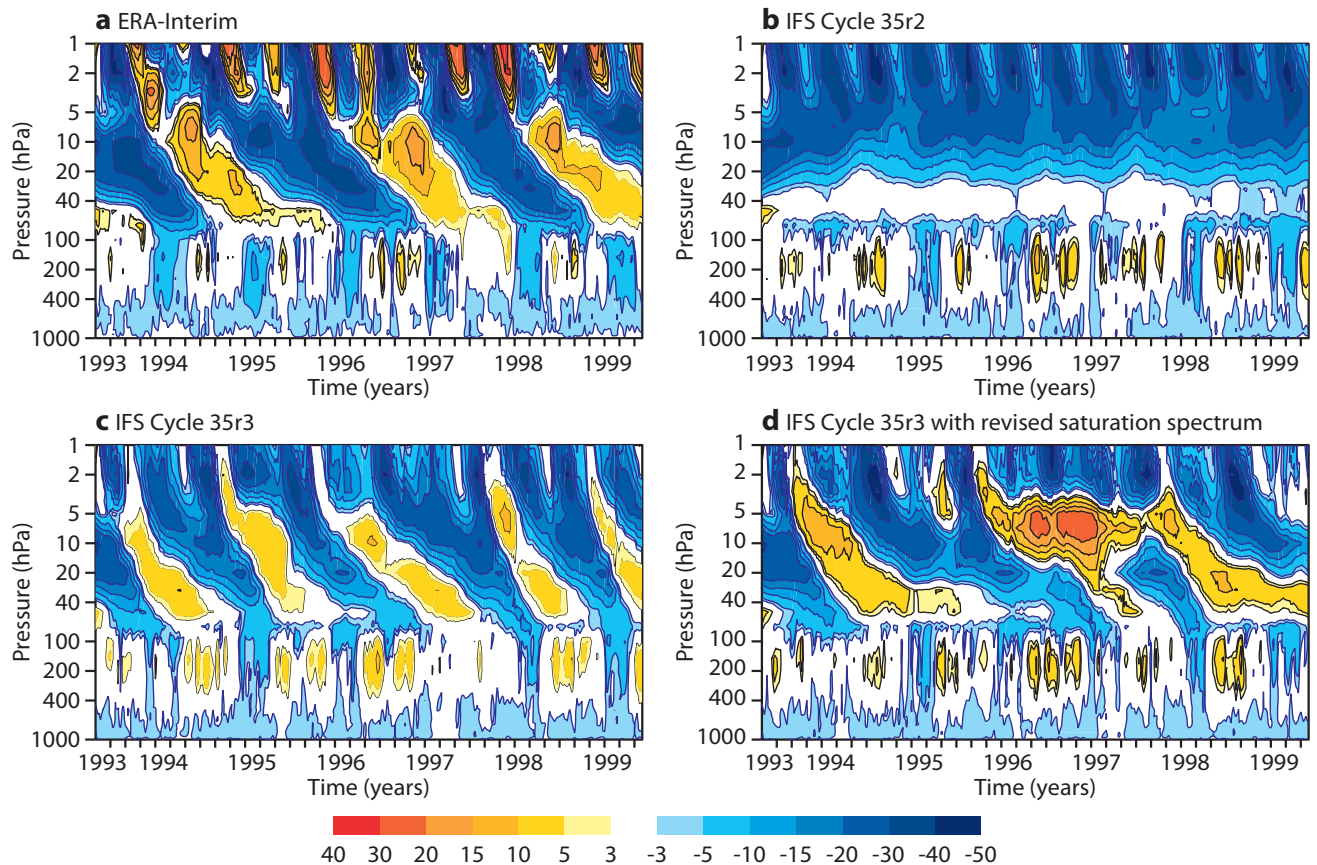


Figure 7 Hovmöller plots (pressure versus time) of the six-year evolution of the zonal wind speed (ms^{-1}) averaged over the tropical band 10°S – 10°N from (a) ERA-Interim, and from six-year integrations with (b) Cy35r2, (c) Cy35r3, and (d) Cy35r3 but with the saturation spectrum for the non-linear gravity wave drag dissipation shifted to higher wavenumbers. ERA-Interim shows a biennial oscillation in the stratosphere, and a semi-annual oscillation in the upper part of the stratosphere and the mesosphere.

Quasi-biennial oscillation

Concerning the variability of the tropical stratosphere, a prominent feature is the quasi-biennial oscillation (QBO) of the zonal wind that is also clearly evident from ERA-Interim (Figure 7a) with amplitudes on the order of $+20$ to -40 ms^{-1} . The quasi semi-annual oscillation of the stratosphere and the lower mesosphere is also present in the reanalysis data. The downward propagation of these oscillations results from breaking gravity waves that deposit momentum near critical levels, thereby changing the zonal winds; this in turn leads to a downward propagation of the critical level.

The ability of the IFS to produce the quasi semi-annual oscillations has been verified with the aid of multi-year integrations. Results for Cy35r2 (Figure 7b), and all previous cycles, show that these cycles have not been able to produce realistic stratospheric oscillations, but instead only produce easterly tropical stratospheric winds that do not propagate downward beyond the 30 hPa level. In contrast, with Cy35r3 (Figure 7c) clear downward propagating oscillations are present with a realistic amplitude that on average extend downward to 60–80 hPa but sometimes even extend to the lower stratosphere and upper troposphere. However, the period of the QBO-like oscillations in Cy35r3 is about 1.3 years, and therefore significantly shorter than that observed.

As shown in Figure 7d, it is possible to simulate the desired period using Cy35r3 by shifting the saturation spectrum in Figure 1 to the right (i.e. to higher wave numbers). These results are consistent with sensitivity studies reported in the literature which showed that shifting the wave saturation, and therefore momentum deposition, to higher levels in the mesosphere leads to a more realistic representation of the period of the QBO. Unfortunately, the latter option could not be retained for the operational cycle Cy35r3 as it leads to problems in the temperature and wind fields at the model top through excessive momentum deposition.

High-resolution analysis suite

The introduction of a parametrization for the non-orographic gravity wave drag, and a more realistic greenhouse gas climatology in Cy35r3 leads to substantial improvements in the mean circulation and variability of the middle atmosphere. These improvements are also evident from pre-operational analysis cycling performed with Cy35r3.

The analysis part of Cy35r3 contains another important contribution to the middle atmosphere. Until Cy35r2 the use of the linearized long-wave radiation scheme has been restricted to the troposphere. This was necessary in order to avoid spurious noise and

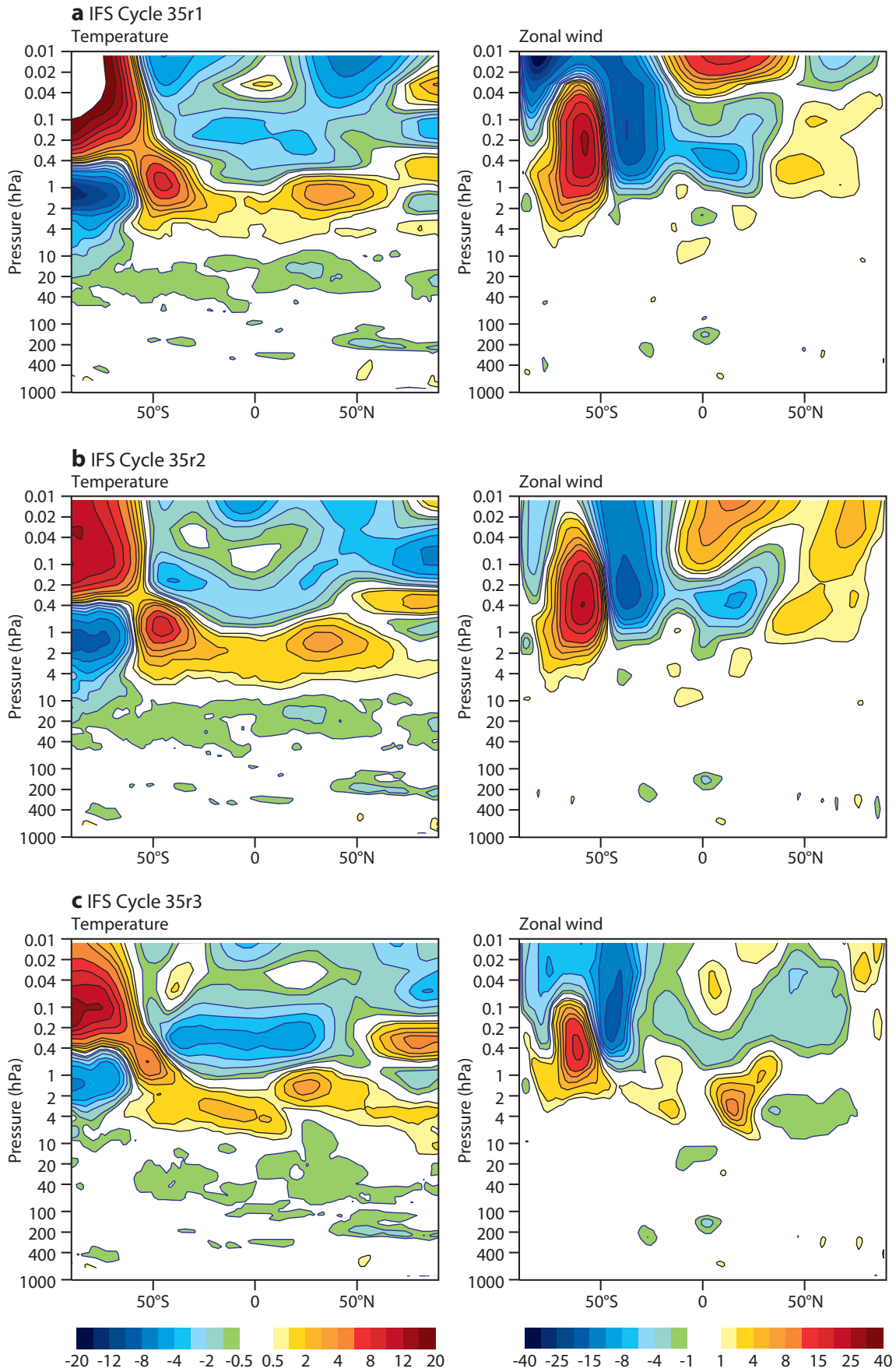


Figure 8 Cross-sections of errors in mean temperature (K, left column) and zonal wind (ms^{-1} , right column) during August 2008 of the 72-hour deterministic high-resolution forecasts with (a) Cy35r1, (b) Cy35r2 and (c) Cy35r3. Each cycle is verified against its own analysis.

deterioration in the tangent linear approximation. However, in Cy35r2 a linearized version of the full long-wave radiation code has been implemented. As this new linear scheme also allows for radiative tendency perturbations in the middle atmosphere, we decided that Cy35r3 should make use of the temperature perturbations due to long-wave radiation throughout the atmosphere. This improves the tangent linear approximation, and makes potentially better use of middle atmosphere observations.

In Figure 8 the mean errors for temperature and zonal wind for August 2008 of the 72-hour deterministic high-resolution T799 (25 km) forecasts with Cy35r1, Cy35r2 and Cy35r3 have been computed with respect to the own analysis of each cycle.

In Cy35r1 (Figure 8a), which was the operational cycle during that period, large model errors existed in the winter mesosphere with mean temperature and wind errors exceeding 20 K and 25 ms⁻¹, respectively. Also the stratopause is apparent as a region with a warm bias of a few K.

In Cy35r2 (Figure 8b) the errors in the upper mesosphere (the uppermost four model layers) have been significantly reduced compared to Cy35r1 due to a better usage of satellite observations the mesosphere with the introduction of the RTTOV9 radiative transfer model.

Finally, with Cy35r3 (Figure 8c) the errors in the mesosphere and upper stratosphere are further reduced. The smaller warm bias around the stratopause, in particular, is due to the new greenhouse gas climatology, whereas the reduction in the mesospheric wind errors has been obtained due to the NOROGWD. There are, however, still problems concerning the upper-stratospheric winds in the tropics, a too strong polar night jet with a too small tilt toward the tropics, and the cold bias in the lower stratosphere has increased by about 0.5 K compared to previous cycles. Overall the medium-range forecast errors with respect to the own analysis are similar to the errors seen in long integrations with respect to SPARC (Figure 4c).

There is some positive impact of Cy35r3 on classical tropospheric scores in the middle latitudes in the medium range. One could expect that, on monthly and seasonal time scales, the middle atmosphere changes, in particular the changes to the polar stratospheric vortex and the more realistic stratospheric oscillations in the tropics, would have an even larger influence on the tropospheric predictions. We do not yet have enough evidence from numerical experimentation to test this hypothesis as currently the improvements in the middle atmosphere analysis and deterministic forecast are not reflected in the operational ensemble monthly and seasonal forecasts

which make use of a 62-level configuration with a model top at 5 hPa.

Further improvements

There is still room for further improving the circulation in the middle atmosphere. One should keep in mind that the NOROGWD scheme uses a globally uniform launch spectrum, and only allows for vertical propagation of gravity waves. It therefore provides a rather simplified representation of the actual generation and oblique propagation of gravity waves. Furthermore, the planned model upgrades in horizontal resolution (late 2009) and vertical resolution (2010) might help to better represent the resolved gravity waves.

Lifting the model top, which in the current high-resolution forecast system is located at the mesopause, could help avoid problems caused by wave reflection from the upper boundary that are noticeable in the tropics. However, an extension of the model into the lower thermosphere would be difficult to realise as it requires modifications to the radiation scheme due to the non-equilibrium radiative processes which become relevant at these altitudes.

Finally, we are also looking forward to the vertical-resolution upgrade of the ensemble prediction system in 2010 which will allow, together with the current physics upgrade, a more realistic representation of the stratosphere/troposphere interactions on monthly to seasonal timescales.

FURTHER READING

- Ern, M., P. Preusse, M.J. Alexander & C.D. Warner**, 2004: Absolute values of gravity wave momentum flux derived from satellite data. *J. Geophys. Res.*, **109**, D20103, doi:10.1029/2004JD004752
- Ern, M., P. Preusse & C.D. Warner**, 2006: Some experimental constraints for spectral parameters used in the Warner and McIntyre gravity wave parameterization scheme. *Atmos. Chem. Phys.*, **6**, 4361–4381.
- Fortuin, J.P.F. & U. Langematz**, 1994: An update on the global ozone climatology and on concurrent ozone and temperature trends. Proceedings SPIE. *Atmos. Sensing and Modelling*, **2311**, 207–216.
- Houghton, J.T., L.G. Meira Filho, B.A. Callander, N. Harris, A. Kattenberg & K. Maskell Eds.**, 1995: IPCC/SACC Climate Change 1995 Report, *Cambridge University Press*.
- Scinoccia, J.F.**, 2003: An accurate spectral nonorographic gravity wave drag parameterization for general circulation models. *J. Atmos. Sci.*, **60**, 667–682.
- Warner, C.D. & M.E. McIntyre**, 1996: On the propagation and dissipation of gravity wave spectra through a realistic middle atmosphere. *J. Atmos. Sci.*, **53**, 3213–3235.
-

The direct assimilation of cloud-affected infrared radiances in the ECMWF 4D-Var

TONY MCNALLY

THERE ARE three major incentives to be able to use cloud-affected infrared radiance observations.

- ◆ The restriction of using only infrared sounding data that can be pre-determined as clear represents a major under-exploitation of very high cost instruments such as the Atmospheric Infrared Sounder (AIRS) and the Infrared Atmospheric Sounding Interferometer (IASI). Estimates of cloud cover vary in the literature, but any instruments with a footprint of order 10 km will typically only yield between 10–30% completely clear soundings.
- ◆ Only using radiances in clear-sky has the potential to bias the assimilation system towards particular synoptic or climatological regions (e.g. areas with low humidity) which may not be representative of the wider atmospheric conditions.
- ◆ There is evidence to suggest that cloudy areas are meteorologically sensitive and that constraining analysis errors in these regions (with observations) is important to limit forecast error growth.

The observed infrared radiance spectra from satellites contain potentially useful information on clouds in addition to the temperature and humidity information they were designed to provide. Cloud parameters have been estimated simultaneously with temperature and humidity in offline retrieval schemes. More recently it has been demonstrated that for weakly affected radiances there is potential to pass externally generated cloud parameters from a 1D-Var retrieval as fixed values to a global direct radiance assimilation scheme. There are significant scientific aspects (discussed in the next section) in which the estimation of cloud parameters differs from the estimation of temperature and humidity. These issues have been addressed in the standalone retrieval algorithms, but as yet have precluded the extension of global operational assimilation schemes such as 4D-Var to estimate cloud parameters from the direct assimilation of cloud-affected infrared radiance data.

Particular issues related to cloud analysis

The assimilation of radiance data (or indeed any observation) may be regarded as a correction process where errors in a background estimate of the atmospheric state are corrected by comparison with the observations. In variational schemes such as 4D-Var, temperature errors in the rather accurate short-range forecast background typically translate into a radiance signal of just a few tenths of a Kelvin – with radiance observation

errors being of a similar magnitude. Signals are slightly larger in the case of humidity, but still typically of order 1 to 2 Kelvin. In contrast, the presence of clouds can easily introduce signals of order many tens of Kelvin in infrared radiance observations and we can see that there is a considerable mismatch between the magnitude of temperature (and humidity) information in the observations compared to the cloud information. While this does not present any theoretical obstacle to the simultaneous estimation of clouds, it does demonstrate the need to be extremely careful when handling the cloud information so as not to destroy the important temperature and humidity information.

Data assimilation schemes require a degree of linearity between the observations and the analysis variables – at least for small perturbations (the so called tangent linear approximation). Put more simply, this requires that the relationship that links the observed quantity (radiances in the case of satellites) to the parameters we wish to estimate in the analysis (e.g. temperature and humidity) should not vary dramatically in different atmospheric conditions. For radiance measured in clear-sky conditions this is reasonably valid. For humidity sensitive radiances the approximation is weaker, but still reasonable. However, in a cloudy sky the dependency on the atmospheric state (i.e. the actual cloud conditions) is potentially extreme. This extreme behaviour means that to exploit the tangent linear approximation within the analysis a very accurate initial description of the cloud conditions is required.

Another potential complication for the inclusion of clouds within the analysis is the availability of background information. For temperature and humidity it has already been stated that the short-range forecast provides rather accurate background information and we have fairly reliable estimates of the error covariance describing this accuracy. Modern NWP models do provide highly detailed cloud information. Also recent satellite missions, such as CLOUDSAT, will certainly improve our understanding and validation of NWP cloud information, but as yet we do not have an accurate quantification or errors for clouds in NWP models.

A further issue relates to matching cloud information provided by the model to the observations. For variables such as temperature a simple interpolation to the observation is sufficient, but for clouds this is potentially more problematic (particularly if there are variable model resolutions involved in the analysis – not representative of the spatial scale of the satellite).

Finally we must consider the issue of how to accurately model the cloud contribution in the infrared radiance data. The most sophisticated and accurate cloudy radia-

tive transfer schemes require inputs of cloud liquid and ice content profiles, cloud fraction profiles and even microphysical parameters that describe the detailed radiative characteristics. In addition, important assumptions must be made about how fractional clouds at each level overlap in the vertical. The next section describes the steps that have been taken to overcome these difficulties.

Extending the 4D-Var analysis for clouds

The analysis has been extended to estimate parameters that describe cloud – namely the cloud top pressure (CP) and the effective cloud fraction (CF). The latter takes into account semi-transparency and represents the equivalent amount of opaque cloud in the instrument field of view. The two extra cloud variables do not exist as spatially continuous fields (as would be the case for example with model fields of temperature or humidity), but as local variables defined and estimated only at satellite observation locations.

The framework used was originally designed to allow the simultaneous analysis of surface parameters from satellite data inside the 4D-Var. It allows different observations with their own particular spatial scales and spectral characteristics to produce independent estimates of quantities such as skin temperature and emissivity – where a single model field would be unlikely to be representative of what the satellite actually observes (e.g. a single NWP model field of skin temperature could not be simultaneously appropriate for microwave and infrared data where the surface penetration depth is very different). In this sense the framework is very suitable for cloud variables where values of the parameters may be strongly dependent on the characteristics of the satellite (e.g. size of the footprint).

Cloud analysis variables handled in this framework are not correlated spatially and explicitly coupled with any other analysis variables through the background

error statistics or the 4D-Var strong model constraint. They are also not transported forward in time to the next assimilation window. However, the estimation of the new cloud variables is strongly constrained by the coupling of clouds and existing analysis variables (such as temperature and humidity) in the radiative transfer simulation of the observed radiances. Background estimates of the additional analysis variables that describe cloud are not taken from the NWP model for the reasons discussed previously. A pragmatic approach has been adopted that uses a small subset of the available radiance channels at a given location to estimate a first guess of the cloud parameters (essentially a least squares fit of CP and CF to the observations).

Selection of overcast data

An important and unique aspect of this scheme is that cloud-affected radiances are only used when the scene is determined to be completely overcast. The justification for this is that many of the problems of analyzing cloud are alleviated when the scene is overcast: difficulties related to the forward modelling of multi-layer clouds and how fractional clouds at different levels overlap in the vertical are removed. The highly simplified cloud analysis variables can be regarded as a good representation of the real cloud conditions. Interactions between surface variables (e.g. skin temperature) and cloud variables in the analysis are removed. Overcast clouds (particularly in the mid to upper troposphere) are most accurately determined by the radiance observations and we may have a high degree of confidence in the accuracy of the background estimate. Finally, we have the possibility of obtaining very high vertical resolution temperature information at the overcast cloud top. Here, many lower-tropospheric and surface sensing radiance channels that would normally (i.e. in clear-sky) provide deep layer temperature information are suddenly only sensitive to a very thin atmospheric

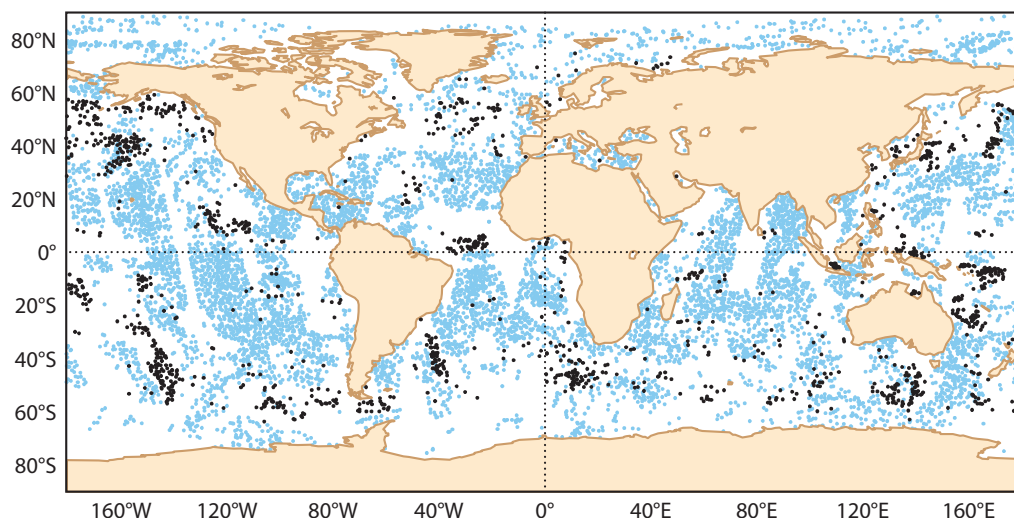


Figure 1 The distribution of overcast cloudy scenes (black dots) and completely clear scenes (blue dots) from the four infrared sensors MetOp-HIRS, NOAA-18 HIRS, MetOp-IASI and AQUA-AIRS during the first 12 hour analysis cycle from 00 UTC on 12 January 2008.

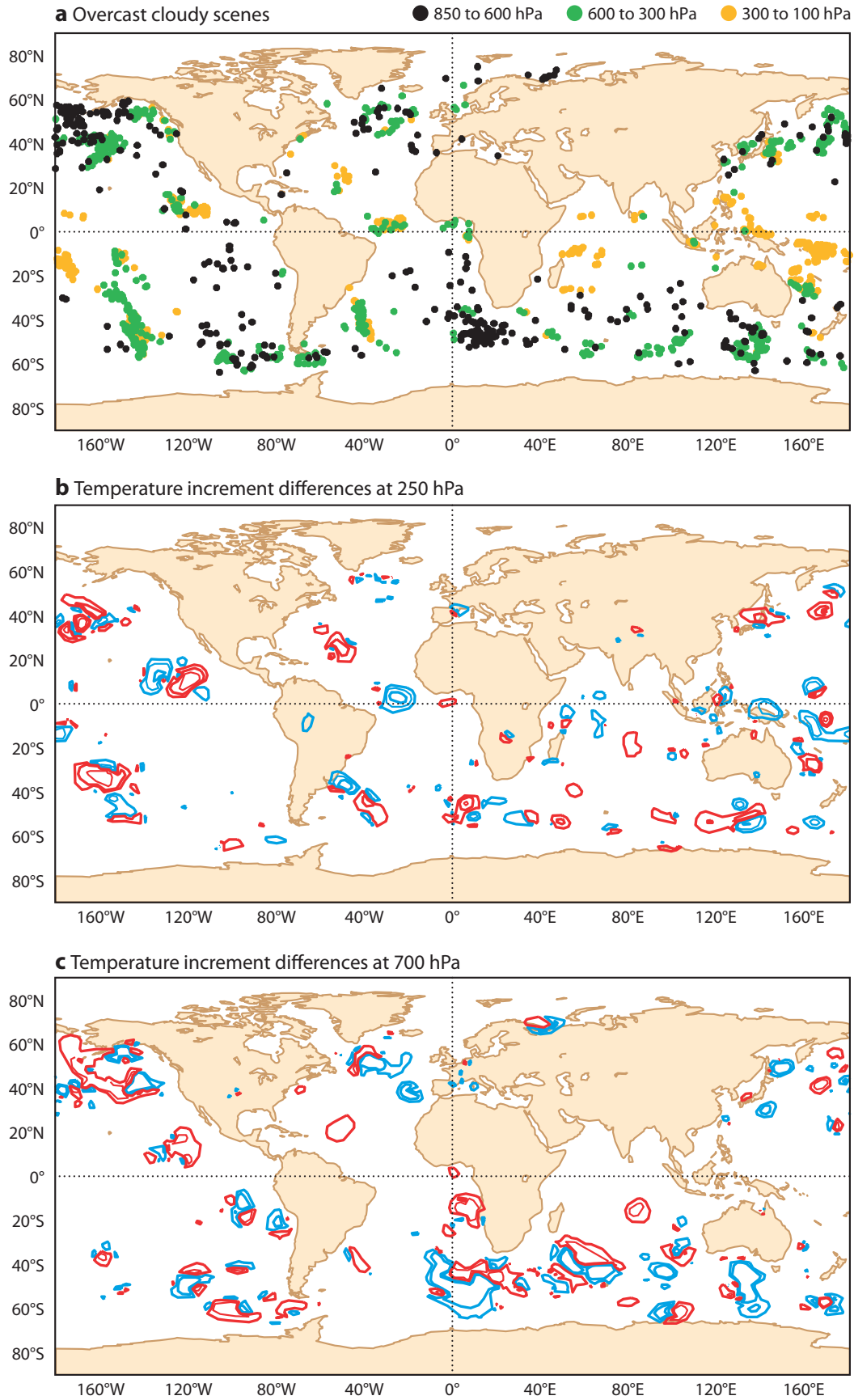


Figure 2 (a) Location of overcast scenes for the first 12-hour analysis cycle (00 UTC on 12 January 2008) separated into three categories depending on cloud height 850 to 600 hPa in black, 600 to 300 hPa in green and 300 to 100 hPa in orange. (b) Temperature increment differences (experiment minus control) at 250 hPa. (c) Temperature increment differences at 700 hPa. For (b) and (c) the contours are at 0.2 K intervals - red contours indicate positive values and blue contours indicate negative values.

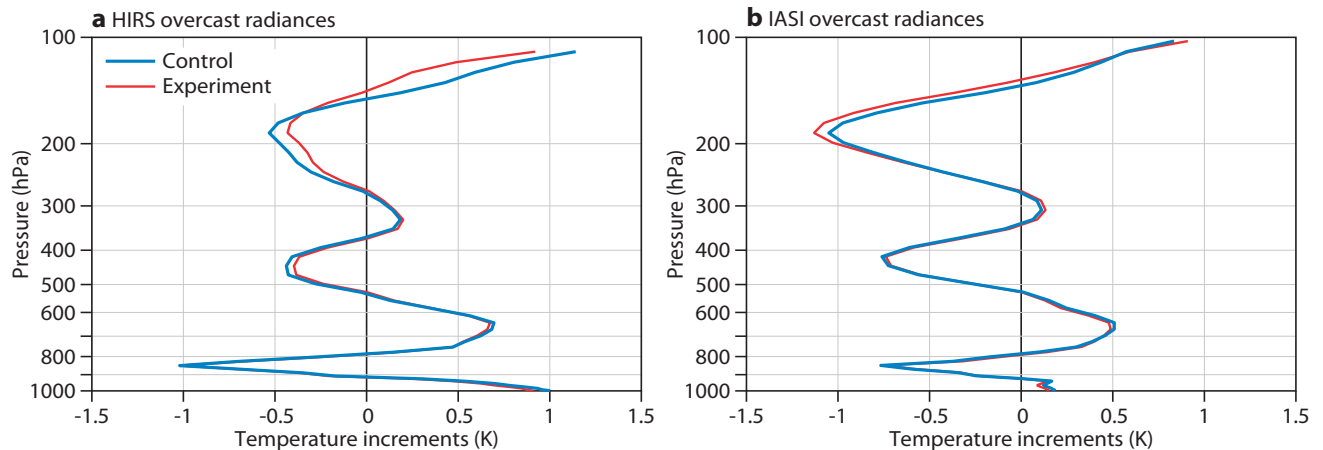


Figure 3 Vertical profiles of temperature increments from (a) HIRS overcast radiances with cloud altitudes diagnosed between 225 and 240 hPa and (b) IASI overcast radiances with cloud altitudes diagnosed between 195 and 215 hPa during the first 12-hour analysis cycle from 00 UTC on 12 October 2008 from two tropical locations east of Papua New Guinea.

layer just above the cloud and together provide a very accurate estimate of its temperature.

Not all overcast scenes are used in the current system. These include cases where the least squares algorithm estimates clouds that are un-physically high, clouds below the surface or clouds with a fraction greater than one (note that no physical bounds are placed as prior constraints upon the algorithm). Overcast scenes when the cloud top is determined to be below 900 hPa are also excluded. While these are quite plausible and physically reasonable, the confidence we may have in the accuracy of low clouds is less and the presence of certain synoptic conditions (such as sharp inversions associated with marine stratocumulus clouds) have proved problematic for convergence in the analysis. Finally, overcast data over land and ice surfaces are not used. While the treatment of overcast data should be insensitive to the underlying surface (as the surface is essentially obscured), a poor prior knowledge of the surface skin temperature or emissivity may cause large errors in the initial cloud parameters and lead to an erroneous identification of a location being overcast.

If the scene is determined as overcast in the initial estimation process the cloud amount is fixed at 1.0. This is obviously sub-optimal as some of the additional information that becomes available in the main analysis may suggest a reduction in the cloud fraction. However, it is a pragmatic measure avoiding the complications of fractional cloud cover. Having fixed the cloud amount, all available channels are then activated in the analysis. The only exceptions are the short-wave channels of HIRS and AIRS which are considered unsuitable as they may have a significantly different cloud sensitivity compared to the long-wave channels (note that no short-wave channels from IASI are currently used at ECMWF).

If the scene is not overcast (or is overcast, but fails to meet the above criteria) the cloud fraction (CF) is fixed at zero and the system reverts to a clear-sky treatment of radiance data – the same as that of the baseline

assimilation. The cloud detection will attempt to find a subset of channels (if any) that are unaffected by the cloud and only these will be activated in the analysis.

Overcast data coverage

An example of the combined additional coverage provided by the use of overcast data from the four infrared sensors is shown in Figure 1 for a typical 12-hour analysis window. For reference the clear-sky data usage is also shown. Overall, the extra overcast data available to the analysis only amounts to approximately 10% of the total. This low yield is mainly due to the stringent quality control criteria that are applied – principally the exclusion of very low clouds (which actually account for the majority of overcast scenes). Nonetheless, it can be seen that the cloudy data that survive the quality control still provide a good filling of gaps in areas where clear-sky radiances are not available. Features such as large frontal regions and the storm tracks are conspicuous, but there is a fairly even distribution of extra data to be found in all areas of the globe.

Analysis increments from overcast radiances

The impact of the overcast infrared radiance data upon the assimilation system has been investigated by examining the difference between analysis increments from a system with clear and overcast data compared to a control system that only uses clear-sky data (shown in Figure 2 for temperature at two levels: 250 hPa and 700 hPa). As expected the increments from the two systems differ in exactly the locations where additional overcast radiance observations are available. Furthermore there is a good correspondence between the altitude where the changes occur and the diagnosed height of the overcast cloud. Above very high clouds the temperature changes are in the upper troposphere and there are no changes lower down. Above low clouds there are temperature changes in the lower troposphere, but these can also be accompanied by differences at upper levels.

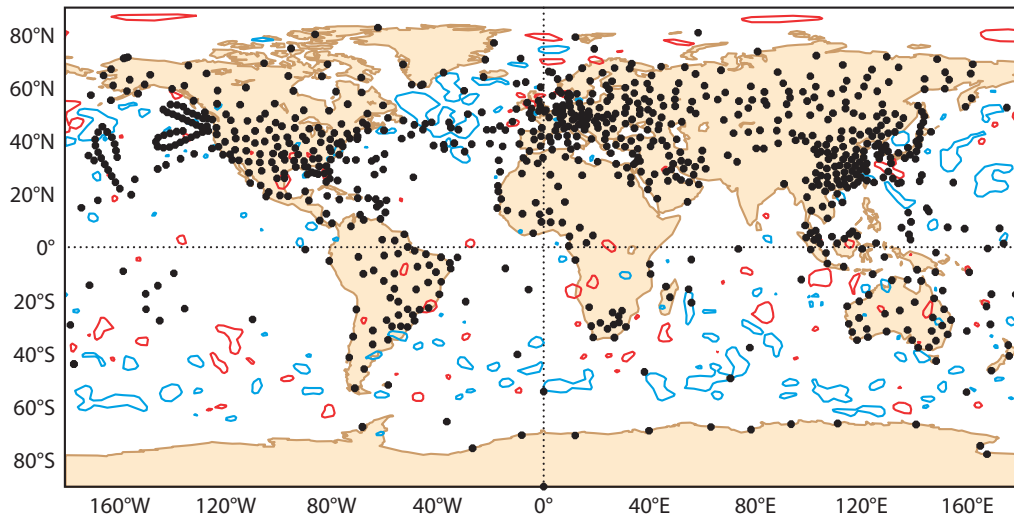


Figure 4 The rms temperature increment differences at 700 hPa (experiment minus control) averaged over the first month of the test period (12 January to 12 February 2008). Blue contours indicate negative values (i.e. where the experiment has smaller rms increments) and red contours indicate the opposite (both contours begin at 0.1 K). Overlaid in black dots are the locations of radiosonde stations reporting and being assimilated at least once during the period.

The correspondence between cloud altitude and the impact of the overcast radiances is better illustrated in Figure 3 where the vertical profile of analysis increments are shown for two locations in the equatorial Pacific (just east of Papua New Guinea). At the first location (Figure 3a) only overcast HIRS radiances are used (above clouds diagnosed at altitudes between 225 and 240 hPa) and at the second location (Figure 3b) only

overcast IASI radiances are used (above clouds diagnosed at altitudes between 195 and 215 hPa). In both cases modified temperature changes at the cloud top are evident, but appear sharper in the case of IASI. While the meteorological conditions at the two locations are not identical (e.g. the clouds at the HIRS location are diagnosed slightly lower than those at the IASI location) we cannot draw too strong a conclusion from this. However, it is a suggestion of what we expect to see – namely higher vertical resolution increments from the advanced infrared sounders compared to HIRS.

While these examples of increment changes demonstrate the ability of the overcast radiances to influence the analysis in a manner (and in regions) that would not be possible with clear-sky data, we need to verify if the increments cause the analysis to move closer to the true atmospheric state. Figure 4 shows temperature increment difference at 700 hPa caused by the assimilation of overcast radiances averaged over a one month period. The shaded areas indicate where the increments are smaller with the overcast data and open contours indicate the opposite. It can be seen that, in the vicinity of isolated oceanic radiosonde observations, the increments of the system using the cloudy data are reduced compared to the clear-sky control (e.g. in the North Atlantic and Pacific and also in the Southern Oceans near Bouvetoya, Crozet, Prince Edward and Kerguelen Islands). Reduced increments at these isolated radiosonde locations indicate that temperature errors are being better constrained in the surrounding oceans where satellite radiances are the dominant source of data. Thus we have some evidence (although the signal is small) that the additional use of overcast radiances is improving the quality of the assimilation with respect to independent observations.

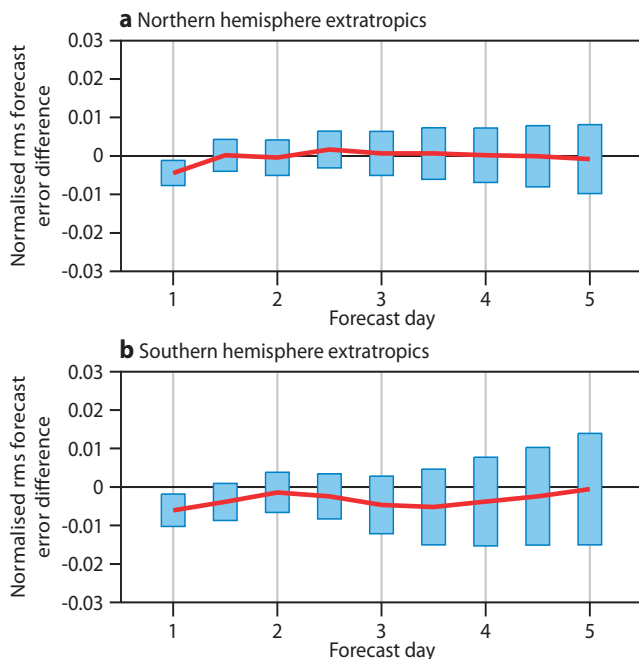


Figure 5 Normalized rms forecast error difference (experiment minus control divided by control) for 500 hPa geopotential height in (a) northern hemisphere extratropics (20°–90°N) and (b) southern hemisphere extratropics (20°–90°S) evaluated over 77 cases from the full test period. Each system is verified against its own analyses and the vertical error bars indicate 95% confidence intervals.

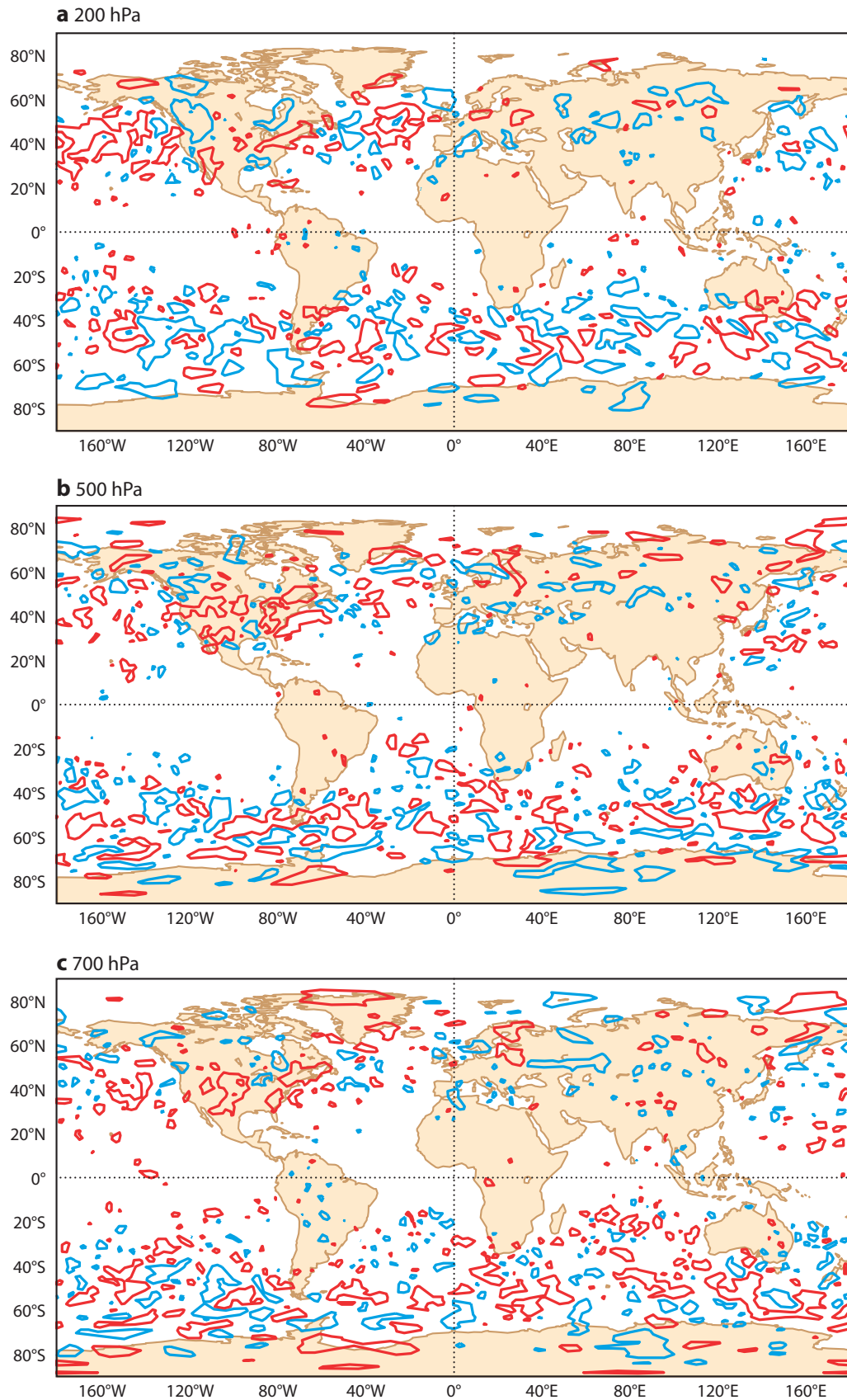


Figure 6 Maps of day five root-mean-square forecast error difference (experiment minus control) for temperature at (a) 200 hPa, (b) 500 hPa and (c) 700 hPa evaluated over 77 cases from the full test period. Each system is verified against its own analysis. Red contours indicate areas where the control forecast error exceeds the experiment by > 0.2 K; blue contours indicate the opposite.

Impact of overcast radiances on forecasts

The impact of using overcast radiance data on forecast quality has been tested over a three-month period. Figure 5 shows a comparison of normalized rms errors (cloudy system minus clear-sky system) for forecasts of 500 hPa geopotential height in the extratropics of the northern and southern hemispheres. Superimposed upon the plot are vertical error bars indicating the statistical significance of the differences evaluated with a standard t-test at the 95% level. In the northern hemisphere the two systems score the same. In the southern hemisphere the average forecast error is reduced using cloudy data, but the statistical significance of the differences is marginal beyond day one.

The geographical distribution of day five temperature forecast error differences averaged over the same three-month period is shown in Figure 6. These demonstrate a positive impact of the overcast radiance data particularly at 200 hPa and 700 hPa in the North Atlantic and North Pacific. The magnitude of the changes in the tropics appears small in these maps, but normalized forecast error differences demonstrate a significant positive impact of the overcast radiances.

Summary and future work

The ECMWF 4D-Var analysis system has been adapted to directly assimilate cloud-affected infrared radiances in addition to the clear-sky data. The extension of the analysis control vector to include simplified cloud parameters allows the estimation of cloud variables simultaneously with all other atmospheric variables. The scheme only assimilates cloud-affected radiances in overcast conditions – thus avoiding many complications associated with the forward modelling and analysis of fractional cloud. In focussing on completely overcast scenes and using all available channels at these locations, this scheme departs from the more traditional approach of trying to use only weak or moderately cloud-affected radiances.

Assimilation experiments have been run with the new scheme in which overcast radiances from HIRS, AIRS and IASI are used in addition to the available clear-sky data. The overcast data locations typically represent 10% or less of the total due to the application of a stringent quality control. The extra data that are used give rise to modified increments (largest for temperature) at and above the diagnosed cloud top. The vertical scales of the temperature changes are much finer than would normally be obtained with clear-sky radiances. Information from independent radiosonde

observations (particularly isolated oceanic stations) suggests that the quality of the assimilation in the mid-lower troposphere is slightly improved using overcast radiances compared to the system that uses only clear data. Forecasts are similarly improved when the overcast radiance data are used.

There are two important issues related to the longer-term future development of this scheme that should be discussed. Firstly, the strict limitation of using only completely overcast situations could be relaxed slightly and modest variations in cloud fraction allowed during the main 4D-Var analysis. This has not been tested so far as the initial emphasis has been placed upon constructing and testing a conservative and robust scheme for use in the operational ECMWF system. Relaxing the overcast limitation will certainly stretch the validity of the simplifying assumptions made here, but the trade off with a higher yield of data may well lead to a better overall system performance. This will be investigated in the near future. The possibility of treating significantly non-overcast situations in this simplified framework is probably rather limited. The description of fractional overlapping cloud would require many additional analysis variables and the estimation of these without reliable independent prior information on clouds (level by level) is likely to be prohibitively under-determined. However, one potential source of information linking the distribution of multilevel clouds is the physical parametrization of the NWP model.

This leads to the second important issue for future development, namely the explicit coupling of the estimated cloud parameters to other atmospheric variables. In its current form the system essentially uses cloud variables as a sink for cloud signal to enable the estimation of temperature and humidity. While the separation of cloud signals is strongly constrained in the main analysis by constraints imposed on temperature and humidity (note this is not the case in a standalone cloudy retrieval), the cloud information is then discarded. However, the knowledge of whether a scene is cloudy or not could (in addition) be digested by the assimilation scheme and lead to thermodynamically consistent adjustment of all atmospheric variables via the adjoint of the model physics. This has already been achieved in the operational use of rain-affected microwave radiance data. Using this as a template, the very acute sensitivity of infrared radiances to cloud may prove to be an additional potent constraint upon the assimilation system in the future.

Peer reviewed publications in 2008

- Balmaseda, M.A., A. Vidard & D.L.T. Anderson**, 2008: The ECMWF Ocean Analysis System: ORA-S3. *Mon. Wea. Rev.*, **136**, 3018–3034
- Balmaseda, M.A., L. Ferranti & F. Molteni**, 2008: The ocean component at ECMWF: towards a seamless prediction system. *CLIVAR Exchanges*, **44**, 36–38
- Bechtold, P., M. Köhler, T. Jung, F. Doblas-Reyes, M. Leutbecher, M.J. Rodwell, F. Vitart & G. Balsamo**, 2008: Advances in simulating atmospheric variability with the ECMWF model: From synoptic to decadal time-scales. *Q. J. R. Meteorol. Soc.*, **134**, 1337–1351
- Bell, W., S.J. English, B. Candy, N. Atkinson, F. Hilton, N. Baker, S.D. Swadley, W.F. Campbell, N. Bormann, G. Kelly & M. Kazumori**, 2008: The assimilation of SSMIS radiances in Numerical Weather Prediction models. *IEEE Trans. Geosci. & Remote Sensing*, **46**, 884–900
- Benedetti, A. and M. Janisková**, 2008: Assimilation of MODIS cloud optical depths in the ECMWF model. *Mon. Wea. Rev.*, **136**, 1727–1746
- Berner, J., F.J. Doblas-Reyes, T.N. Palmer, G. Shutts and A. Weisheimer**, 2008: Impact of a cellular automaton backscatter scheme on the systematic error and seasonal prediction skill of a global climate model. *Philos. Trans. R. Soc.*, **A366**, 2561–2579
- Branković, Č, B. Matjačić, S. Ivatek-Šahdan & R. Buizza**, 2008: Dynamical downscaling of ECMWF ensemble forecasts for cases of severe weather: ensemble statistics and cluster analysis. *Mon. Wea. Rev.*, **136**, 3323–3342
- Buizza, R.**, 2008: The value of probabilistic prediction. *Atmos. Sci. Lett.*, **9**, 36–42, doi: 10.1002/asl.170
- Buizza, R.**, 2008: Comparison of a 51-member low-resolution (TL399L62) ensemble with a 6-member high-resolution (TL799L91) lagged-forecast ensemble. *Mon. Wea. Rev.*, **136**, 3343–3362
- Casado, M.J., M.A. Pastor & F.J. Doblas-Reyes**, 2008: Euro-Atlantic circulation types and modes of variability in winter. *Theor. Appl. Climatol.*, **94**, 8, 10.1007/s00704-008-0036-2
- Ferro, C.A.T., D.S. Richardson & A.P. Weigel**, 2008: On the effect of ensemble size on the discrete and continuous ranked probability scores. *Meteorol. Appl.*, **15**, 19–24
- Gutierrez, J.M., C. Primo, M.A. Rodriguez & J. Fernandez**, 2008: Spatiotemporal characterization of ensemble prediction systems – the Mean-Variance of Logarithms (MVL) diagram. *Nonlinear Processes Geophys.*, **15**, 109–114
- Hagedorn, R., T.M. Hamill & J.S. Whitaker**, 2008: Probabilistic forecast calibration using ECMWF and GFS ensemble reforecasts. Part I: Two-metre temperatures. *Mon. Wea. Rev.*, **136**, 2608–2619
- Hagedorn, R., T.M. Hamill & J.S. Whitaker**, 2008: Probabilistic forecast calibration using ECMWF and GFS ensemble reforecasts. Part II: Precipitation. *Mon. Wea. Rev.*, **136**, 2620–2632
- Holmes, T., M. Drusch, J.-P. Wigneron & R. de Jeu**, 2008: A global simulation of microwave emission: Error structures based on output from ECMWF's operational Integrated Forecast System. *IEEE Trans. Geosci. & Remote Sensing*, **46**, 846–856
- Iversen, T., J. Kristiansen, T. Jung & J. Barkmeijer**, 2008: Optimal atmospheric forcing perturbations for the Cold Ocean Warm Land pattern. *Tellus A*, **60A**, 528–546
- Fernández, J., C. Primo, A.S. Cofiño, J.M. Gutiérrez & M.A. Rodríguez**, 2008: MVL spatiotemporal analysis for model intercomparison in EPS: application to the DEMETER multi-model ensemble. *Clim. Dyn.*, doi: 10.1007/s00382-008-0456-9
- Jolliffe, I.T. & C. Primo**, 2008: Evaluating rank histograms using decompositions of the chi-square test statistic. *Mon. Wea. Rev.*, **136**, 2133–2139
- Jung, T. & M. Leutbecher**, 2008: Scale-dependent verification of ensemble forecasts. *Q. J. R. Meteorol. Soc.*, **134**, 973–984
- Kelly, G., P. Bauer, A. Geer, P. Lopez & J.-N. Thépaut**, 2008: Impact of SSM/I observations related to moisture, clouds and precipitation on global NWP forecast skill. *Mon. Wea. Rev.*, **136**, 2713–2726
- Leutbecher, M. & T.N. Palmer**, 2008: Ensemble forecasting. *J. Comput. Phys.*, **227**, 3515–3539
- Orr, A. & P. Bechtold**, 2008: Improvement in the capturing of short-range warm season orographic precipitation in the ECMWF model. *Meteorol. Atmos. Phys.*, **99**, doi: 10.1007/s00703-008-0288
- Palmer, T.N., F.J. Doblas-Reyes, A. Weisheimer & M. Rodwell**, 2008: Towards “seamless” prediction: Calibration of climate-change projections using seasonal forecasts. *Bull. Am. Meteorol. Soc.*, **89**, 459–470
- Pappenberger, F., J. Bartholmes, J. Thielen, H.L. Cloke, R. Buizza & A. de Roo**, 2008: New dimensions in early flood warning across the globe using grand-ensemble weather predictions. *Geophys. Res. Lett.*, **35**, L10404, doi: 10.1029/2008GL33837
- Pappenberger, F., K. Scipal & R. Buizza**, 2008: Hydrological aspects of meteorological verifications. *Atmos. Sci. Lett.*, **9**, 43–52, (doi: 10.1002/asl.171)
- Parker, D.J., A. Fink, S. Janicot, J.-B. Ngamini, M. Douglas, E. Afiesimama, A. Agusti-Panareda, A. Beljaars, F. Dide, A. Diedhiou, T. Lebel, J. Polcher, J.-L. Redelsperger, C. Thorncroft & D.J. Posselt, G.L. Stephens & M. Miller**, 2008: CLOUDSAT: Adding a new dimension to a classical view of extratropical cyclones. *Bull. Am. Meteorol. Soc.*, **89**, 5, 599–609

Primo, C., M.A. Rodriguez & J.M. Gutierrez, 2008: Logarithmic bred vectors. A new ensemble method with adjustable spread and calibration time. *J. Geophys. Res.*, **113**, D05116,

Ringer, M. & S.B. Healy, 2008: Monitoring twenty-first century climate using GPS radio occultation bending angles. *Geophys. Res. Lett.*, **35**, L05708, doi:10.1029/2007GL032468

Scipal, K., M. Drusch & W. Wagner, 2008: Assimilation of a ERS scatterometer derived soil moisture index in the ECMWF numerical weather prediction system. *Adv. Water Resources*, **31**, 1101–1112

Tan, D.G.H., E. Andersson, J. deKloe, G.-J. Marseille, A. Stoffelen, P. Poli, M.-L. Denneulin, A. Dabas, D. Huber, O. Reitebuch, P. Flamant, O. Le Rille & H. Nett, 2008: The ADM-Aeolus wind retrieval algorithms. *Tellus A*, **60A**, 191–205

Thielen, J., J. Schaake, R. Hartman & R. Buizza, 2008: Aims, challenges and progress of the Hydrological Ensemble Prediction Experiment (HEPEX) – a summary of the 3rd HEPEX workshop held in Stresa 27–29 June 2007. *Atmos. Sci. Lett.*, **9**, 29–35, doi: 10.1002/asl.168

Wedi, N.P. & P.K. Smolarkiewicz, 2008: A reduced model of the Madden-Julian Oscillation. *Int. J. Numer. Methods Fluids*, **56**, 1583–1588

Wilson, G.A., 2008: The AMMA radiosonde programme and its implications for the future of atmospheric monitoring over Africa. *Bull. Am. Meteorol. Soc.*, **89**, 1015–1027

Woollings, T., B.J. Hoskins, M. Blackburn & P. Berrisford, 2008: A new Rossby wave-breaking interpretation of the North Atlantic Oscillation. *J. Atmos. Sc.*, **65**, 609–626

ECMWF Calendar 2009

Sep 7–10	Seminar on "Diagnosis of Forecasting and Data Assimilation Systems"	Oct 13–14	Policy Advisory Committee (28 th Session)
Sep 14–16	ESF Exploratory Workshop on 'Improved Quantitative Fire Description with Multi-species Inversions of Observed Plumes'	Oct 19	Advisory Committee of Co-operating States (15 th Session)
Sep 30–Oct 2	Scientific Advisory Committee (38 th Session)	Nov 2–6	12 th Workshop on "Meteorological Operational Systems"
Oct 7–9	Technical Advisory Committee (40 th Session)	Nov 9–11	ECMWF/GLASS Workshop on 'Land Surface Modelling, Data Assimilation and the Implications for Predictability'
Oct 12–16	Training Course – Use and interpretation of ECMWF products for WMO Members	Nov 23–26	Workshop on 'Monitoring Atmospheric Composition and Climate (MACC)'
Oct 12–13	Finance Committee (83 rd Session)	Dec 8–9	Council (72 nd Session)

ECMWF publications

(see <http://www.ecmwf.int/publications/>)

Technical Memoranda

- 593 **Orr, A.**: The representation of non-orographic gravity waves in the IFS. Part II: A physically based spectral parametrization. *May 2009*
- 592 **Orr, A. & N. Wedi**: The representation of non-orographic gravity waves in the IFS. Part I: Assessment of the middle atmosphere climate with Rayleigh friction. *May 2009*
- 591 **Anderson, D.L.T., F.J. Doblas-Reyes, M. Balmaseda & A. Weisheimer**: Decadal variability: processes, predictability and prediction. *May 2009*
- 590 **Flemming, J., A. Inness, H. Flentje, V. Huijnen, P. Moinat, M.G. Schultz & O. Stein**: Coupling global chemistry transport models to ECMWF's integrated forecast system. *May 2009*
- 589 **Bauer, P.**: 4D-Var Assimilation of MERIS total column water vapour retrievals over land. *April 2009*
- 588 **Janssen, P.A.E.M. & J.-R. Bidlot**: On the extension of the freak wave warning system and its verification. *May 2009*
- 587 **Inness, A., J. Flemming, M. Suttie & L. Jones**: GEMS data assimilation system for chemically reactive gases. *May 2009*

Index of past newsletter articles

This is a selection of articles published in the *ECMWF Newsletter* series during the last five years. Articles are arranged in date order within each subject category. Articles can be accessed on the ECMWF public website – www.ecmwf.int/publications/newsletter/index.html

	No.	Date	Page		No.	Date	Page
NEWS				NEWS			
71 st Council session on 25–26 June	120	Summer 2009	3	Collaboration with the Executive Body of the Convention on Long-Range Transboundary Air Pollution	103	Spring 2005	24
EUMETNET's 'Oslo Declaration'	120	Summer 2009	3	25 years since the first operational forecast	102	Winter 2004/05	36
Operational assimilation of Indian radiosondes	120	Summer 2009	4	COMPUTING			
Assimilation of IASI in NWP	120	Summer 2009	5	ARCHIVING, DATA PROVISION AND VISUALISATION			
Goodbye GEMS – Hello MACC	120	Summer 2009	6	New Automated Tape Library for the Disaster Recovery System	113	Autumn 2007	34
Ocean waves at ECMWF	120	Summer 2009	7	The next generation of ECMWF's meteorological graphics library – Magics++	110	Winter 2006/07	36
ECMWF Annual Report for 2008	120	Summer 2009	7	COMPUTERS, NETWORKS, PROGRAMMING, SYSTEMS FACILITIES AND WEB			
Forecast Products Users' Meeting, June 2009	120	Summer 2009	8	The EU-funded BRIDGE project	117	Autumn 2008	29
Diagnostics of data assimilation system performance	120	Summer 2009	9	ECMWF's Replacement High Performance Computing Facility 2009-2013	115	Spring 2008	44
Philippe Bougeault leaves ECMWF	119	Spring 2009	3	Improving the Regional Meteorological Data Communications Network (RMDCN)	113	Autumn 2007	36
RMetS recognises the achievements of Adrian Simmons and Tim Palmer	119	Spring 2009	4	New features of the Phase 4 HPC facility	109	Autumn 2006	32
A new Head of Research for ECMWF	119	Spring 2009	4	Developing and validating Grid Technology for the solution of complex meteorological problems	104	Summer 2005	22
ERA-Interim for climate monitoring	119	Spring 2009	5	Migration of ECFS data from TSM to HPSS ('Back-archive')	103	Spring 2005	22
The Call Desk celebrates 15 years of service	119	Spring 2009	6	METEOROLOGY			
ECMWF Seminar on the 'Diagnosis of Forecasting and Data Assimilation Systems'	119	Spring 2009	7	OBSERVATIONS AND ASSIMILATION			
ERA-40 article designated as a 'Current Classic'	119	Spring 2009	7	Solar biases in the TRMM microwave imager (TMI)	119	Spring 2009	18
Weather forecasting service for the Dronning Maud Land Air Network (DROMLAN)	119	Spring 2009	8	Variational bias correction in ERA-Interim	119	Spring 2009	21
ECMWF's plans for 2009	118	Winter 2008/09	2	Towards the assimilation of ground-based radar precipitation data in the ECMWF 4D-Var	117	Autumn 2008	13
Use of high performance computing in meteorology	118	Winter 2008/09	5	Progress in ozone monitoring and assimilation	116	Summer 2008	35
Atmosphere-Ocean Interaction	118	Winter 2008/09	6	Improving the radiative transfer modelling for the assimilation of radiances from SSU and AMSU-A stratospheric channels	116	Summer 2008	43
Use of GIS/OGS standards in meteorology	118	Winter 2008/09	8	ECMWF's 4D-Var data assimilation system – the genesis and ten years in operations	115	Spring 2008	8
Additional ERA-Interim products available	118	Winter 2008/09	9	Towards a climate data assimilation system: status update of ERA-Interim	115	Spring 2008	12
ECMWF workshops and scientific meetings in 2009	118	Winter 2008/09	10	Operational assimilation of surface wind data from the Metop ASCAT scatterometer at ECMWF	113	Autumn 2007	6
ECMWF Education and Training Programme 2009	117	Autumn 2008	2	Evaluation of the impact of the space component of the Global Observing System through Observing System Experiments	113	Autumn 2007	16
GRAS SAF Workshop on applications of GPS radio occultation measurements	117	Autumn 2008	4	Data assimilation in the polar regions	112	Summer 2007	10
PREVIEW Data Targeting System (DTS)	117	Autumn 2008	5	Operational assimilation of GPS radio occultation measurements at ECMWF	111	Spring 2007	6
Verification of severe weather forecasts	117	Autumn 2008	6	The value of targeted observations	111	Spring 2007	11
GMES Forum, 16-17 September 2008	117	Autumn 2008	7	Assimilation of cloud and rain observations from space	110	Winter 2006/07	12
Exploratory analysis and verification of seasonal forecasts with the KNMI Climate Explorer	116	Summer 2008	4	ERA-Interim: New ECMWF reanalysis products from 1989 onwards	110	Winter 2006/07	25
Optimisation and improvements to scalability of 4D-Var for Cy33r2	116	Summer 2008	6	Analysis and forecast impact of humidity observations	109	Autumn 2006	11
Operational assimilation of GRAS measurements at ECMWF	116	Summer 2008	7	Surface pressure bias correction in data assimilation	108	Summer 2006	20
First meeting of the TAC Subgroup on the RMDCN	115	Spring 2008	2	A variational approach to satellite bias correction	107	Spring 2006	18
Signing of the Co-operation Agreement between ECMWF and Latvia	115	Spring 2008	4				
Two new Co-operation Agreements	114	Winter 2007/08	4				
Signing of the Co-operation Agreement between ECMWF and Montenegro	114	Winter 2007/08	7				
New High Performance Computing Facility	114	Winter 2007/08	13				
Fifteenth anniversary of EPS	114	Winter 2007/08	14				
Co-operation Agreement signed with Morocco	110	Winter 2006/07	9				
Co-operation Agreement with Estonia	106	Winter 2005/06	8				
Long-term co-operation established with ESA	104	Summer 2005	3				
Co-operation Agreement with Lithuania	103	Spring 2005	24				

	No.	Date	Page		No.	Date	Page
OBSERVATIONS AND ASSIMILATION				OCEAN AND WAVE MODELLING			
"Wavelet" J_b – A new way to model the statistics of background errors	106	Winter 2005/06	23	NEMOVAR: A variational data assimilation system for the NEMO ocean model	120	Summer 2009	17
New observations in the ECMWF assimilation system: satellite limb measurements	105	Autumn 2005	13	Climate variability from the new System 3 ocean reanalysis	113	Autumn 2007	8
The direct assimilation of cloud-affected infrared radiances in the ECMWF 4D-Var	120	Summer 2009	32	Progress in wave forecasts at ECMWF	106	Winter 2005/06	28
CO ₂ from space: estimating atmospheric CO ₂ within the ECMWF data assimilation system	104	Summer 2005	14	Ocean analysis at ECMWF: From real-time ocean initial conditions to historical ocean analysis	105	Autumn 2005	24
Sea ice analyses for the Baltic Sea	103	Spring 2005	6	High-precision gravimetry and ECMWF forcing for ocean tide models	105	Autumn 2005	6
The ADM-Aeolus satellite to measure wind profiles from space	103	Spring 2005	11	ENVIRONMENTAL MONITORING			
An atlas describing the ERA-40 climate during 1979–2001	103	Spring 2005	20	Smoke in the air	119	Spring 2009	9
Planning of adaptive observations during the Atlantic THORPEX Regional Campaign 2003	102	Winter 2004/05	16	GEMS aerosol analyses with the ECMWF Integrated Forecast System	116	Summer 2008	20
FORECAST MODEL				Progress with the GEMS project	107	Spring 2006	5
Improvements in the stratosphere and mesosphere of the IFS	120	Summer 2009	22	A preliminary survey of ERA-40 users developing applications of relevance to GEO (Group on Earth Observations)	104	Summer 2005	5
Parametrization of convective gusts	119	Spring 2009	15	The GEMS project – making a contribution to the environmental monitoring mission of ECMWF	103	Spring 2005	17
Towards a forecast of aerosols with the ECMWF Integrated Forecast System	114	Winter 2007/08	15	METEOROLOGICAL APPLICATIONS AND STUDIES			
A new partitioning approach for ECMWF's Integrated Forecast System	114	Winter 2007/08	17	EPS/EFAS probabilistic flood prediction for Northern Italy: the case of 30 April 2009	120	Summer 2009	10
Advances in simulating atmospheric variability with IFS cycle 32r3	114	Winter 2007/08	29	Use of ECMWF lateral boundary conditions and surface assimilation for the operational ALADIN model in Hungary	119	Spring 2009	29
A new radiation package: McRad	112	Summer 2007	22	Using ECMWF products in global marine drift forecasting services	118	Winter 2008/09	16
Ice supersaturation in ECMWF's Integrated Forecast System	109	Autumn 2006	26	Record-setting performance of the ECMWF IFS in medium-range tropical cyclone track prediction	118	Winter 2008/09	20
Towards a global meso-scale model: The high-resolution system T799L91 and T399L62 EPS	108	Summer 2006	6	The ECMWF 'Diagnostic Explorer': A web tool to aid forecast system assessment and development	117	Autumn 2008	21
The local and global impact of the recent change in model aerosol climatology	105	Autumn 2005	17	Diagnosing forecast error using relaxation experiments	116	Summer 2008	24
Improved prediction of boundary layer clouds	104	Summer 2005	18	ECMWF's contribution to AMMA	115	Spring 2008	19
Two new cycles of the IFS: 26r3 and 28r1	102	Winter 2004/05	15	Coupled ocean-atmosphere medium-range forecasts: the MERSEA experience	115	Spring 2008	27
ENSEMBLE PREDICTION AND SEASONAL FORECASTING				Probability forecasts for water levels in The Netherlands	114	Winter 2007/08	23
EUROSIP: multi-model seasonal forecasting	118	Winter 2008/09	10	Impact of airborne Doppler lidar observations on ECMWF forecasts	113	Autumn 2007	28
Using the ECMWF reforecast dataset to calibrate EPS forecasts	117	Autumn 2008	8	Ensemble streamflow forecasts over France	111	Spring 2007	21
The THORPEX Interactive Grand Global Ensemble (TIGGE): concept and objectives	116	Summer 2008	9	Hindcasts of historic storms with the DWD models GME, LMQ and LMK using ERA-40 reanalyses	109	Autumn 2006	16
Implementation of TIGGE Phase 1	116	Summer 2008	10	Hurricane Jim over New Caledonia: a remarkable numerical prediction of its genesis and track	109	Autumn 2006	21
Predictability studies using TIGGE data	116	Summer 2008	16	Recent developments in extreme weather forecasting	107	Spring 2006	8
Merging VarEPS with the monthly forecasting system: a first step towards seamless prediction	115	Spring 2008	35	MERSEA – a project to develop ocean and marine applications	103	Spring 2005	21
Seasonal forecasting of tropical storm frequency	112	Summer 2007	16	Starting-up medium-range forecasting for New Caledonia in the South-West Pacific Ocean – a not so boring tropical climate	102	Winter 2004/05	2
New web products for the ECMWF Seasonal Forecast System-3	111	Spring 2007	28	A snowstorm in North-Western Turkey 12–13 February 2004 – Forecasts, public warnings and lessons learned	102	Winter 2004/05	15
Seasonal Forecast System 3	110	Winter 2006/07	19	Early medium-range forecasts of tropical cyclones	102	Winter 2004/05	7
The ECMWF Variable Resolution Ensemble Prediction System (VAREPS)	108	Summer 2006	14				
Limited area ensemble forecasting in Norway using targeted EPS	107	Spring 2006	23				
Ensemble prediction: A pedagogical perspective	106	Winter 2005/06	10				
Comparing and combining deterministic and ensemble forecasts: How to predict rainfall occurrence better	106	Winter 2005/06	17				
EPS skill improvements between 1994 and 2005	104	Summer 2005	10				
Ensembles-based predictions of climate change and their impacts (ENSEMBLES Project)	103	Spring 2005	16				

Useful names and telephone numbers within ECMWF

Telephone

Telephone number of an individual at the Centre is:
 International: +44 118 949 9 + three digit extension
 UK: (0118) 949 9 + three digit extension
 Internal: 2 + three digit extension
 e.g. the Director's number is:
 +44 118 949 9001 (international),
 (0118) 949 9001 (UK) and 2001 (internal).

	Ext
Director	
Dominique Marbouty	001
Deputy Director & Head of Operations Department	
Walter Zwiefelhofer	003
Head of Research Department	
Erland Källén	003
Head of Administration Department	
Ute Dahremöller	007
<hr/>	
Switchboard	
ECMWF switchboard	000
Advisory	
Internet mail addressed to Advisory@ecmwf.int Telefax (+44 118 986 9450, marked User Support)	
Computer Division	
<i>Division Head</i>	
Isabella Weger	050
<i>Computer Operations Section Head</i>	
Sylvia Baylis	301
<i>Networking and Computer Security Section Head</i>	
Rémy Giraud	356
<i>Servers and Desktops Section Head</i>	
Richard Fisker	355
<i>Systems Software Section Head</i>	
Neil Storer	353
<i>User Support Section Head</i>	
Umberto Modigliani	382
<i>User Support Staff</i>	
Paul Dando	381
Dominique Lucas	386
Carsten Maaß	389
Pam Prior	384
Christian Weihrauch	380
Computer Operations	
<i>Call Desk</i>	303
<i>Call Desk email:</i> calldesk@ecmwf.int	
<i>Console – Shift Leaders</i>	803
<i>Console fax number</i> +44 118 949 9840 <i>Console email:</i> newops@ecmwf.int	
<i>Fault reporting – Call Desk</i>	303
<i>Registration – Call Desk</i>	303
<i>Service queries – Call Desk</i>	303
<i>Tape Requests – Tape Librarian</i>	315

E-mail

The e-mail address of an individual at the Centre is:
 firstinitial.lastname@ecmwf.int
 e.g. the Director's address is: D.Marbouty@ecmwf.int
 For double-barrelled names use a hyphen
 e.g. J-N.Name-Name@ecmwf.int

Internet web site

ECMWF's public web site is: <http://www.ecmwf.int>

	Ext
Meteorological Division	
<i>Division Head</i>	
Erik Andersson	060
<i>Meteorological Applications Section Head</i>	
Alfred Hofstadler	400
<i>Data and Services Section Head</i>	
Baudouin Raoult	404
<i>Graphics Section Head</i>	
Stephan Siemen	375
<i>Meteorological Operations Section Head</i>	
David Richardson	420
<i>Meteorological Operations Room</i>	
Meteorological Operations Analyst	427
Meteorological Operations Assistant	426
Data Division	
<i>Division Head</i>	
Jean-Noël Thépaut	030
<i>Data Assimilation Section Head</i>	
Lars Isaksen	852
<i>Satellite Data Section Head</i>	
Peter Bauer	080
<i>Re-Analysis Section Head</i>	
Dick Dee	352
Probabilistic Forecasting & Diagnostics Division	
<i>Division Head</i>	
Tim Palmer	600
<i>Seasonal Forecasting Section Head</i>	
Franco Molteni	108
Model Division	
<i>Division Head</i>	
Martin Miller	070
<i>Numerical Aspects Section Head</i>	
Agathe Untch	704
<i>Physical Aspects Section Head</i>	
Anton Beljaars	035
<i>Ocean Waves Section Head</i>	
Peter Janssen	116
GMES Coordinator	
Adrian Simmons	700
Education & Training	
Renate Hagedorn	257
ECMWF library & documentation distribution	
Els Kooij-Connally	751

© Copyright 2009

European Centre for Medium-Range Weather Forecasts, Shinfield Park, Reading, RG2 9AX, England

Literary and scientific copyright belong to ECMWF and are reserved in all countries. This publication is not to be reprinted or translated in whole or in part without the written permission of the Director. Appropriate non-commercial use will normally be granted under condition that reference is made to ECMWF.

The information within this publication is given in good faith and considered to be true, but ECMWF accepts no liability for error, omission and for loss or damage arising from its use.